

1 **Hidden paleosols on a high-elevation Alpine plateau (NW Italy):**
2 **evidence for Lateglacial Nunatak?**

3 Pintaldi E.¹, D'Amico M.^{1,2}, Colombo N.^{1,2,3,*}, Martinetto E.³, Said-Pullicino D.¹, Giardino M.³,
4 Freppaz M.^{1,2}

5 ¹Università degli Studi di Torino - DISAFA, Largo Paolo Braccini 2, 10095, Grugliasco (TO), Italy

6 ²Università degli Studi di Torino, NATRISK, Research Centre on Natural Risks in Mountain and Hilly Environments,
7 Largo Paolo Braccini 2, 10095, Grugliasco (TO), Italy

8 ³Università degli Studi di Torino - DST, Via Valperga Caluso, 35, 10125 Torino (TO), Italy

9 *Correspondence to: nicola.colombo@unito.it (N. Colombo)

10

11 **Abstract**

12 Alpine soils can provide valuable paleo-environmental information, representing a powerful tool for
13 paleoclimate reconstruction. However, since Pleistocene glaciations and erosion-related processes
14 erased most of the pre-existing landforms and soils, reconstructing soil and landscape development
15 in high-mountain areas can be a difficult task. In particular, a relevant lack of information exists on
16 the transition between the Last Glacial Maximum (LGM ~21,000 yr BP) and the Holocene (~11,700
17 yr BP), with this climatic shift that plays a crucial role for environmental thresholds identification.
18 The present study aims at reconstructing the history and origin of hidden paleosols inside periglacial
19 blockstreams and blockfields on a high-elevation Alpine plateau (Stolenberg Plateau) above 3000 m
20 a.s.l., in the Northwestern Italian Alps. The results indicate that these soils recorded the main warming
21 climatic phases occurred from the end of the LGM until the Late Holocene ~4,000 yr BP. Our
22 reconstructions, together with the high carbon stocks of these paleosols, suggest that during warming
23 phases the environmental conditions on the Plateau were suitable for plant life and pedogenesis,
24 already since 22,000-21,000 yr BP. These paleosols reasonably evidence the existence of a
25 Lateglacial Nunatak representing, to our knowledge, one of the first documented relict non-glacial

26 surfaces in the high-elevated European Alps. Thus, the Stolenberg Plateau provides important
27 information about past climate and surface processes since the end of LGM, suggesting new
28 perspectives on the long-term landscape evolution of the high European Alps.

29

30 **Keywords:** ^{14}C dating, $\delta^{13}\text{C}$, blockstream/blockfield, paleoclimate, Umbrisol, relict surface

31

32 **Introduction**

33 High-mountain areas can preserve traces of dramatic climatic variations, representing unique
34 geosites and “storytellers” about the past landscape dynamics (Favilli et al., 2008). However,
35 reconstructing soil and landscape evolution in such areas can be a difficult task because Pleistocene
36 glaciations and related processes erased most of the pre-existing landforms and soils, leading to the
37 formation of a complex mosaic of Quaternary sediments and soils of different ages (Sartori et al.,
38 2001). Nevertheless, on scattered stable surfaces preserved during Pleistocene glaciations, ancient
39 soils can be locally preserved for long periods (D’Amico et al., 2016). These soils, apparently in
40 contrast with Holocene soil forming conditions, represent paleosols (when buried) or relict soils
41 (Ruellan, 1971) that constitute excellent pedo-signatures of different specific past environmental
42 conditions.

43 Relict surfaces are recognizable as flat summits and plateaus perched high above the valley floors
44 at different elevations, in which erosion and deposition processes were very limited (D’Amico et al.,
45 2016), because of lateral migration of glacial masses (Carraro and Giardino, 2004). Those surfaces
46 that were not affected by the passage of glaciers experienced extreme cold conditions, which induced
47 strong frost-action processes (e.g., frost-shattering, frost sorting, frost heave, etc.) (Karte, 1983),
48 leading to the formation of periglacial features such as blockfields, blockstreams, and tors
49 (Goodfellow, 2007; Ballantyne, 2010). Because of their high stability on certain poorly weatherable
50 materials (D’Amico et al., 2019), these Pleistocene relict periglacial landforms are considered key

51 indicators of ancient non-glacial surfaces (Goodfellow, 2007). Therefore, they have been used in
52 paleoclimatic reconstructions, as their formation can be associated with specific past environmental
53 conditions (e.g., Karte, 1983; Wilson, 2013; D'Amico et al., 2019). In particular, blockfields, which
54 are usually associated with mountain summits and plateaus, have been used as paleo-indicators of
55 nunataks (e.g., Ballantyne and Harris, 1994; Ballantyne, 1998, 2010) or non-erosive ice covers such
56 as cold-based glaciers (e.g., Nesje et al., 1988; Kleman and Borgström, 1990; Hättestrand and
57 Stroeven, 2002).

58 Nunataks (Dahl, 1987) are isolated hills or mountain peaks that projected above the ice shields and
59 alpine-type icecap (Fairbridge, 1968). They have been proposed as possible biological refugia during
60 glacial periods (Schönswetter et al., 2005; Goodfellow, 2007; Birks and Willis, 2008), serving as
61 sources for the rapid reoccupation of the later deglaciated landscape (Fairbridge, 1968). While several
62 studies have been focused on nunataks especially at high latitudes (e.g., Birks, 1994; McCarroll et al.,
63 1995; Ballantyne et al., 1998; Kullman, 2008), there is a paucity of such works in the European Alps
64 (Schönswetter et al., 2005; Carcaillet and Blarquez, 2017; Carcaillet et al., 2018), likely due to
65 intrinsic difficulties in finding relict surfaces preserved from glaciations. Moreover, although many
66 studies proposed paleoclimatic reconstructions in Alpine environments, they were mostly localized
67 at elevation lower than 2200 m a.s.l. and in different climatic conditions (e.g., Kerschner and Ochs,
68 2008; Samartin et al., 2012a; Heiri et al., 2014). Furthermore, while the environmental changes from
69 the Oldest Dryas to the Holocene are relatively well documented (e.g., Samartin et al., 2012b; Cossart
70 et al., 2012, Heiri et al., 2014), a substantial gap of paleoclimate data during the transition between
71 Last Glacial Maximum (LGM) and the Early Lateglacial still exists in the Alps, despite the well
72 reported beginning of deglaciation, which occurred no later than 22,000-18,000 yr BP (Ivy-Ochs et
73 al., 2006a; Ivy-Ochs, 2015, Monegato et al., 2017; Seguinot et al., 2018).

74 In 2017, on a high-elevation Alpine plateau (Stolenberg Plateau) covered by periglacial features
75 (blockstreams and blockfields), at 3030 m a.s.l., thick and well-developed Umbrisols were detected.
76 Despite the large stony cover and the extreme sparse vegetation, these soils showed carbon stocks

77 comparable to alpine tundra or even forest soils (Pintaldi et al., 2021). Considering the high elevation,
78 the specific morphology, the presence of large periglacial features and the well-developed soils within
79 them, we hypothesize that the Plateau may represent an Alpine Nunatak on which ancient paleosols
80 have been preserved. If these soils are truly paleosols, what their age could be? What is the origin of
81 the soil organic carbon stored within them? If this soil organic carbon was not allochthonous (e.g.
82 transported by wind or through atmospheric deposition), what kind of vegetation could grow at the
83 time of soil formation? If the Plateau preserved very old paleosols, could it represent an Alpine
84 Nunatak and what could have been the history of the past evolution of such high-elevated landscape?

85 Based on these considerations, this work aims at investigating the age and origin of soils
86 discovered within blockstreams and blockfields (Pintaldi et al., 2021), through the application of plant
87 remains investigation, plant fragments and soil ^{14}C dating, and soil $\delta^{13}\text{C}$ analysis. Moreover, based
88 on the interpretation of the obtained results and literature data, the work aims at reconstructing the
89 possible paleoenvironmental evolution of this high-elevated periglacial landscape since the end of the
90 LGM.

91

92 **2. Materials and Methods**

93 **2.1 Study Site**

94 The Stolenberg Plateau (3030 m a.s.l.) is located at the foot of the southern slope of Monte Rosa
95 (4634 m a.s.l.), along the border between Valle d'Aosta and Piemonte regions, NW Italian Alps
96 (Long-Term Ecological Research-LTER site Istituto Mosso, 45°52'42.87"N, 7°52'0.64"E) (Fig. 1,
97 Supplementary material 1). The Plateau has a south-east orientation and covers a surface of ca. 1.35
98 ha, with a slope angle between 0° and 13°. Meteorological parameters of the study area (air
99 temperature and total liquid precipitation) were recorded by the Bocchetta delle Pisse Automatic
100 Weather Station (AWS) (2401 m a.s.l., managed by ARPA Piemonte), located ca. 2.5 km east of the
101 study area (on the same slope). The temperatures at the Plateau were obtained using the standard lapse

102 rate of $6\text{ }^{\circ}\text{C km}^{-1}$. The mean cumulative annual snowfall was recorded by the Col d'Olen AWS (2901
103 m a.s.l., managed by the Italian Army, Comando Truppe Alpine - Servizio Meteomont), located ca.
104 500 m south-east of the Plateau. The LTER area has a total annual precipitation of ca. 1300 ± 270 mm
105 (1997-2019) at 2400 m a.s.l., with a winter minimum and a late spring-summer maximum. The
106 Plateau has a mean annual air temperature of $-2.4\pm 0.7\text{ }^{\circ}\text{C}$ (1988-2019) and a mean summer (June,
107 July, August) air temperature of $4.4\pm 1.3\text{ }^{\circ}\text{C}$; July is the warmest month, with a mean air temperature
108 of $5.2\pm 2.7\text{ }^{\circ}\text{C}$. The mean annual liquid precipitation is ca. 358 ± 86 mm (1997-2019) while the mean
109 cumulative annual snowfall is ca. 800 ± 143 cm, with a snow cover lasting for at least 8 months (2008-
110 2019).

111 The Plateau is covered by a thick layer of stones of variable size (from decimetric to metric), well
112 organized in autochthonous blockfields, blockstreams/sorted stripes, gelifluction lobes, tilted stones,
113 and weakly developed sorted circles (Pintaldi et al., 2021). No glacial striations or roches moutonnées
114 have been detected on the few highly fractured rock outcrops. The parent material is composed of
115 gneiss and mica-schists (Monte Rosa nappe, Penninic basement), and metabasites (Zermatt-Saas unit)
116 (Tognetto et al., 2021). The vegetation cover, which is almost absent or confined to small patches,
117 reaching no more than 5% of the Plateau surface, is composed of alpine species such as *Silene acaulis*,
118 *Carex curvula*, *Salix herbacea* in the vegetated patches, while *Festuca halleri*, *Poa alpina*,
119 *Ranunculus glacialis*, *Leucanthemopsis alpina*, *Cerastium uniflorum*, *Oxyria digyna* and a few other
120 scattered species grow also in the stone-covered area.

121 In 2017, during operational activities for constructing a new cableway station on the Plateau, three
122 soil trenches were opened in the construction area close to the protected geosite (soil profiles P1, P2,
123 and P3 in Fig. 1), revealing surprisingly well-developed soils under the stony cover. These soils were
124 characterized by dark and thick organic C-rich A horizons (Fig. 2), and were classified as Skeletic
125 Umbrisol (Arenic, Turbic), according to IUSS Working Group WRB (2015). Soil texture was
126 generally loamy sand or sandy loam, pH (measured in H_2O) values were extremely to moderately
127 acidic and carbonates were absent. Total Organic Carbon (TOC) content reached maximum values

128 of ca. 20 g kg⁻¹ in the A horizons of profiles P1 and P2 and over 10 g kg⁻¹ in profile P3; the soil C
129 stocks (up to ~ 5 kg m⁻²) were comparable to vegetated or even forest soils, despite the extremely
130 sparse vegetation cover (Pintaldi et al., 2021). Geophysical investigations indicated that these hidden
131 soils were widespread on the Plateau. Moreover, no relevant permafrost bodies have been detected in
132 the site, even though some permafrost patches cannot be excluded (Pintaldi et al., 2021). The detailed
133 description of the soil profiles, as well as their physical and chemical properties, distribution, and
134 thickness, are reported in Pintaldi et al. (2021). The ground surface thermal regime monitoring (2019-
135 2020) showed no significantly negative soil temperatures under the blockstreams (Supplementary
136 material 2, Fig. S1,2). However, during the snow-free season, soil temperatures under these
137 periglacial features were colder than in nearby snowbed soils covered by vegetation (Supplementary
138 material 2, Fig. S3, Tab. S1).

139
140
141

142 **2.2. Plant remains analysis**

143 The presence of few plant fragments mixed within the soil material was observed within soil samples
144 collected from the umbric A horizons in the soil profiles. In order to isolate and identify the plant
145 fragments within soil matrix, to reconstruct the possible past vegetation of the Plateau, a plant
146 macroremains approach was adopted, starting from the assumption that plant material contained in
147 paleosols may preserve the main features of soil "seed banks" (Ter Heerd et al., 1996). Furthermore,
148 the investigation was applied on two additional soil samples collected deep inside a soil-filled rock
149 wedge (a vertical fracture in the substrate filled with vertically stratified soil materials, likely formed
150 by freeze-thaw action), at 3 m depth (Fig. 3) along the southern border of the plateau (site "Wedge"
151 in Fig. 1). We used the method for extraction of seeds and fruits from deep time sediments (e.g.,
152 Martinetto and Vassio, 2010), because recent experiences (Bertolotto et al., 2012) on a few soils

153 showed that this was effective. Soil samples were processed in the laboratory with a very dilute
154 solution of H₂O₂ (1%–3%), applied to disaggregate the biotic from the abiotic components and
155 facilitate the floatation of the lighter and porous particles, usually fruits and seeds. Subsequently, the
156 floating particles and the heavier materials that settled to the bottom were gently washed and sieved
157 separately. After this material was dried and sorted by size, the fruits, seeds, and plant fragments were
158 picked from the sieved residue. These were analyzed under a stereomicroscope and taxa were
159 identified using atlases of recent fruits and seeds (Berggren, 1969, 1981; Bojnansky and Fargašova,
160 2007; Ercole et al., 2012); atlases of fossil fruits and seeds (Velichkevich and Zastawniak, 2006,
161 2009); and by comparison to the Modern Carpological Collection (MCC) at the Department of Earth
162 Sciences at the University of Torino. Finally, these identifications were compiled into a database, and
163 abundance data were generated based on fruit and seed counts.

164

165

166 **2.3. Plant fragments and soil ¹⁴C dating**

167 Radiocarbon dating (¹⁴C) was performed on six plant fragment samples, accurately selected after
168 the plant macroremains investigation: five samples, consisting of recognizable but fossil-resembling
169 plant fragments (dark coloured, mineral coatings), were obtained from soil samples collected in the
170 umbric A horizons (usually in the 0-10 cm layer); one sample, consisting of unrecognizable plant
171 fragments (strongly decomposed), derived from soil samples collected in the soil wedge at 3 m depth.

172 Furthermore, ¹⁴C radiocarbon dating was performed on ten soil samples, nine of which selected
173 from soil profiles: two from profile P1 (1,2), four from P2 (7,8,9,9bis) and three from P3 (2,3,5) (Fig.
174 1); one sample was collected in the only fully vegetated patch of the plateau (P4), at 10-20 cm depth
175 (A horizon) (Fig. 1). The radiocarbon dating was performed at CEDAD, the Centre for Applied
176 Physics, Dating and Diagnostics, Department of Mathematics and Physics “Ennio de Giorgi” -
177 University of Salento, Lecce, Italy, using radiocarbon accelerator mass spectrometry (AMS) analysis

178 (Calcagnile et al., 2005) and the standard preparation methods (D'Elia et al., 2004). Radiocarbon
179 dates of soil samples were calibrated in calendar age by using the software OxCal v. 4.4.4 Bronk
180 Ramsey (2021) (Figs. S4-S8), based on atmospheric data (Reimer et al., 2020). Further
181 methodological details can be found in Supplementary material 3. Radiocarbon dating of soils and
182 sediments can be problematic due to the presence of pre-aged carbon (e.g., Lowe and Walker, 2000;
183 Pessenda et al., 2001; Thorn et al., 2009) or fresh/allochthonous organic matter (Wang et al., 1996;
184 Tonneijck et al., 2006). Therefore, terrestrial plant macrofossils have been considered the most
185 reliable material for ^{14}C dating (Lowe and Walker, 2000; Hatté et al., 2001). However, the fossil
186 record of the Alpine flora is generally scarce due to the lack of conditions suitable for the
187 accumulation of macro-remains at the highest elevations (Lang, 1994). If materials such as charcoal,
188 wood, or other plant macrofossils (Muhs et al., 2003) are lacking, dating of soils or sediments is
189 generally accepted (Wang et al., 2014), especially in specific sites and under certain conditions (Lowe
190 and Walker, 2000). Thus, the interpretation of ^{14}C dates must be adapted to the specific soil ecosystem
191 under study (Tonneijck et al., 2006).

192

193 **2.4. Soil $\delta^{13}\text{C}$ stable isotope signature**

194 The soil $\delta^{13}\text{C}$ signatures are frequently used to reconstruct plant community history and the sources
195 of soil organic carbon (Bai et al., 2012). To verify the typical $\delta^{13}\text{C}$ signature of present-day vegetated
196 soils in the study area, which clearly reflects the existing vegetation (Meyer et al., 2014), soil samples
197 were collected from the A horizons (~10 cm depth) of five vegetated permanent study sites at slightly
198 lower elevation (Fig. S3) in the LTER site (2750-2900 m a.s.l.): four from typical snow-bed
199 community belonging to the *Salicion herbaceae* phytosociological alliance (site 1,2,6,8) and one from
200 an alpine microthermal *Carex curvula*-dominated grassland, ascribable to the Caricion curvulae
201 alliance (site 3). These soils were classified as Skeletic Regosols, Cambisols or Umbrisols (Magnani
202 et al., 2017; Freppaz et al., 2019). The analysis was performed also on fourteen selected soil samples

203 collected at the Plateau: two from profile P1 (1,2), five from profile P2 (7,8,9,9bis,13,15), five from
204 profile P3 (1,2,3,4,5) and one from the vegetated patch P4 (10-20 cm depth, corresponding to the A
205 horizon). The detailed scheme and description of sampling point within soil profiles under
206 blockstreams/blockfields was described in Pintaldi et al. (2021). Samples were air-dried, sieved to 2
207 mm and checked using stereomicroscope to eventually remove macro-contaminants. Then samples
208 were ground and sieved to 0.5 mm. The $\delta^{13}\text{C}$ signature of total organic carbon (due to the absence of
209 carbonates) was directly determined using an Isoprime 100 continuous flow stable isotope mass
210 spectrometer coupled to a Vario Isotope Select elemental analyzer (EA-IRMS; Elementar
211 Analysensysteme GmbH, Hanau, Germany). The $\delta^{13}\text{C}$ -values (‰) were calibrated relative to the
212 international standard Vienna Pee Dee Belemnite (VPDB) by means of a three-point calibration using
213 standard reference materials IAEA-600, IAEA-603 and IAEA-CH3. Measurement uncertainty was
214 monitored by repeated measurements of internal laboratory standards and standard reference
215 materials. Precision was determined to be ± 0.1 ‰ based on repeated measurements of calibration
216 standards and internal laboratory standards. Accuracy was determined to be ± 0.1 ‰ on the basis of
217 the difference between the observed and known δ values of check standards and their standard
218 deviations. The total analytical uncertainty for $\delta^{13}\text{C}$ values was estimated to be ± 0.2 ‰. Significant
219 differences (p -value < 0.05) in $\delta^{13}\text{C}$ values between present-day vegetated soils and soils under
220 periglacial features were evaluated through one-way analysis of variance (ANOVA) combined with
221 Tukey HSD test. Statistical analyses were performed using R software, v. 3.6.0 (R Core Team, 2019).

222

223 **3. Results**

224 **3.1. Plant remains and ^{14}C dating**

225 The quantity of plant fragments found in the soils was very scarce, representing a negligible
226 fraction compared to the soil matrix. However, they were composed of remains with definite
227 morphologies, including cm-sized leaves (consisting mainly of well-preserved and recognizable

228 specimens of *Salix herbacea*, *Cerastium uniflorum* and *Poaceae* sp.) and mm-sized fruits and seeds,
229 which have been mostly identified as belonging to taxa growing today in surrounding snowbed areas
230 and in the small vegetated patch on the Plateau (Tab. 1, Fig. 1). Only in sample F, which was collected
231 inside the wedge (Fig. 3), the degree of decomposition was much higher, so that the morphology of
232 larger plant fragments was vague and not recognizable. Only a few tiny fruits and seeds still had
233 diagnostic morphologies and allowed the identification of some plant taxa (Tab. 1)

234 Concerning radiocarbon dating, the plant fragment samples were all modern (after 1950 AD, Tab.
235 2), except the strongly decomposed sample F, which was dated back to 1,796-1,571 cal. yr BP (Tab
236 2, Fig. 4A).

237

238 **3.2. Soil Organic Matter ^{14}C dating and $\delta^{13}\text{C}$ signature**

239 Unlike plant fragments, the results from AMS on soil samples revealed a wide range of ages,
240 covering several thousands of years and different well-distinct climatic periods, between ca. 22,000-
241 21,000 yr and 4,400-4,100 cal. yr BP (Tab. 2, Fig. 4). All radiocarbon dates were rounded and here
242 presented as calibrated radiocarbon ages (cal. yr BP = years before 1950 A.D.). In P1 the age of soil
243 samples was related with depth, in fact the oldest samples P1-1, dated between 8,787 and 8,434 cal.
244 yr BP (Tab. 2, Fig. 4B), was located close to the lower boundary of the umbric A horizon, while the
245 youngest one (P1-2), dated between 5,744 and 5,583 yr cal. BP, was located close to the surface
246 stones-soil interface (Fig. 2 A1-A2). In P2 the age of the samples was not related to depth: the oldest
247 sample P2-9, dated between 17,536-17,014 and 18,228-17,870 (P2-9bis) cal. yr BP (Fig. 4C) (values
248 obtained from two independent and blind datings performed in different moments), was located close
249 to the surface stones-soil interface, while the stable organic C in C-rich cryoturbated patches (P2-7),
250 located close to the lower boundary of the umbric A horizon, was much younger (6,500-6,306 cal. yr
251 BP) (Fig. 2 B1-B2); the central and rather homogeneous part of the A horizon (P2-8) dates back to
252 8,534-8,302 cal. yr BP. In P3 the age of the samples was not related to depth as well: the oldest

253 samples P3-2 and P3-3, dating back to 18,916-18,611 and 22,168-21,431 cal. yr BP respectively
254 (Tab.2, Fig. 4D), were taken from homogeneous materials in the central part of the umbric horizon,
255 while a younger radiocarbon age was obtained in the deeper part of the A horizon, close to the lower
256 boundary (sample P3-5, Fig. 2 C1-C2), dating back to 13,337-13,110 cal. yr BP (Fig. 4E). The
257 youngest soil sample, P4, taken from the A horizon in the currently fully vegetated patch, was dated
258 between 4,405 and 4,090 cal. yr BP (Tab. 2, Fig. 4F).

259 The $\delta^{13}\text{C}$ signature of present-day vegetated soils provided by EA-IRMS ranged between -23.3
260 (Site 1) and -25.7 ‰ (Site 3), with a mean value of -24.2 ‰ (+/-1.1) (Tab. 3). The $\delta^{13}\text{C}$ of soil samples
261 from the Plateau showed very similar values, ranging between -23.5 (P3-3) and -24.7 ‰ (P1-1), with
262 a mean of -24.1 ‰ (+/- 0.4), while the soil sample collected from the vegetated patch (P4) had a
263 slightly greater value of $\delta^{13}\text{C}$ of -22.7 ‰ (Tab. 3). No significant differences were detected between
264 present-day vegetated soils and soils under periglacial features ($p < 0.05$, Tukey HSD-test, Fig. 5).

265

266 **4. Discussion**

267 **4.1 Plant fragments ^{14}C dating**

268 The plant fragment samples were generally modern (Tab. 2), except sample F, which was dated
269 between 1,796 and 1,571 yr BP, corresponding therefore to the small warm phase occurred during
270 the Roman time (Mercalli, 2004). The strong difference in age between sample F and the other
271 samples was already reflected in the different degree of decomposition, as the larger plant fragments
272 in sample F were not recognizable. This sample, collected at ca. 3 m depth below the present-day
273 surface inside a rock wedge, evidenced strongly active periglacial processes, sufficient to activate the
274 rock wedge and thus its filling by surface soil material in the following centuries. This indicates that
275 cryoturbation processes acted across millennia, strongly mixing plant fragments within the soil
276 matrix, until they became unrecognizable. The presence of modern plant fragments within the soil
277 matrix, although very scarce, can be explained mainly by the aeolian transport from the surrounding

278 vegetated surfaces. The plant material could have been trapped by the stone layer and moved towards
279 the soil surface through the large spaces between the rocks. Alternatively, a small input from the
280 sporadically occurring vegetation growing within the stones may have contributed.

281

282 **4.2 Soil ^{14}C dating**

283

284 Differently from plant samples, datings of the soil samples collected from the Plateau covered an
285 extended time interval, involving both Pleistocene and Holocene epochs. If some kind of very old-
286 aged material (i.e. from LGM or even older) was deposited on the Plateau surface (i.e. derived from
287 depositions on a cold-based glacier or by wind), it should have been deposited also on the nearby
288 glacier surfaces. However, similar old-aged organic materials have never been detected in the well-
289 studied Monte Rosa glaciers (Jenk et al., 2009; Thevenon et al., 2009). Currently, the oldest date
290 obtained from an ice core, collected at ~80 m depth on the nearby Colle Gnifetti, was around 15,000
291 yr (Jenk et al., 2009). In the European Alps, on glacier surfaces, the most important source for the
292 deposition of already aged organic materials is soil dust (Hoffman, 2016), a large part of which is
293 originated from Saharan dust storm (e.g., Wagenbach and Geis, 1989; Wagenbach et al., 1996;
294 Hoffman, 2016). The age of organic matter in these atmospheric depositions range between 1,000
295 and 5,000 yr (Eglinton et al., 2002; Jenk et al., 2006), with a mean of ca. 2,500 (Hoffman, 2016).
296 Finally, the contribution of anthropogenic emissions was also considered as a possible cause for the
297 aging of samples (Jenk et al., 2006), the so-called Suess effect (Suess, 1955). However, this effect is
298 generally negligible on samples older than 2,000-5,000 yr BP (Graven et al., 2015; Köhler, 2016).
299 Therefore, most of our samples, especially the oldest ones, were out of the range of influence of the
300 Suess effect.

301 Based on the previous considerations, our soil samples cannot therefore be influenced by other
302 than local organic carbon sources (i.e. vegetation grown during warming phases). Furthermore, the

303 soil texture of the paleosols at the Stolenberg Plateau was loamy sand or sandy loam and no
304 differences were found among profiles and between surface and deep samples (Pintaldi et al., 2021),
305 thus rejecting also the hypothesis of a Loess deposition, which is otherwise mainly composed of silt-
306 sized material dominated by quartz (Smalley et al., 2006), but could also include organic matter.

307 The surface position of the oldest samples and the general inversion of the typical age-depth
308 relationship can be explained by the strong cryoturbation processes occurring on the Plateau,
309 especially during the cold climatic phases. Indeed, cryoturbation processes mix and displace soil
310 horizons (Bockheim and Tarnocai, 1998; Pintaldi et al., 2016), redistributing organic matter (e.g., van
311 Vliet-Lanoë et al., 1998; Hormes et al., 2004; Bockheim, 2007). Furthermore, other works reported
312 inverted soil age-depth relationship (e.g., Carcaillet, 2001; Favilli et al., 2008; Egli et al., 2009; Serra
313 et al., 2020), as the young and contemporary carbon can be transported by soil turbation processes,
314 such as cryoturbation and bioturbation, thus contributing to the rejuvenation of the subsoil
315 (Scharpenseel and Becker-Heidmann, 1992; Rumpel et al., 2002; Favilli et al., 2008). Besides the
316 well-developed periglacial features, cryoturbation processes were also evidenced by the internal soil
317 morphology, which showed inclusions of surface A-horizon materials at depth, as well as strong
318 convolutions and block displacement above wedges (Pintaldi et al., 2021).

319 Remarkably, ages similar to the ones of our oldest samples have never been detected in soils at
320 such high-elevated ecosystems in the European Alps. For instance, Baroni and Orombelli (1996)
321 found a Cambisol with buried A horizons at Tisa Pass (3200 m a.s.l.), but with a radiocarbon age of
322 around 6,400-6300 yr BP, while Orombelli (1998) obtained an age up to ca. 9,000 yr BP (2500 m
323 a.s.l.) for the Rutor Peat Bog. Glacier basal sediments at the Jamtalfener and Stubai glaciers (Austria)
324 had ages around 17,000 and 22,000 yr BP, respectively (Hoffman, 2016). Furthermore, although at
325 lower elevation (2100 m a.s.l.), Favilli et al. (2008, 2009) obtained comparable ages (17,000-18,000
326 yr BP) for an Entic Podzol, in the alpine belt in NE Italy. Other comparable radiocarbon ages (~21,000
327 yr BP) were reported by Carcaillet and Blarquez (2017) for a tree refugium at ~2200 m a.s.l., in the
328 Western Alps.

329 Our soils could have experienced several different climatic conditions, retaining information about
330 past climates, ranging from the end of the LGM (Ivy-Ochs, 2015) to the beginning of the Late
331 Holocene (Walker et al., 2012), when a progressive cooling happened since ~4,000 yr BP (Deline
332 and Orombelli, 2005; Orombelli et al., 2005). All the detected ages matched exactly and exclusively
333 with the main warming phases/interstadials occurring from the LGM until the transition between the
334 Holocene Climatic Optimum (HCO) and the Late Holocene (:), whereas no soil samples from cold
335 phases/stadials were detected (further details in chapter 5).

336

337 **4.3 Soil $\delta^{13}\text{C}$ signature**

338 The overall $\delta^{13}\text{C}$ signature of present-day vegetated soils obtained by the stable isotope analysis,
339 was comparable to those reported for soils and alpine vegetation in high-elevation ecosystems
340 (Körner, 2003; Körner et al., 2016). The $\delta^{13}\text{C}$ signatures of soils under periglacial features
341 corresponded very well with those of present-day vegetated soil (Tab. 3), thus indicating that the soil
342 organic carbon probably originated from alpine plants with the same isotopic signature of present-
343 day vegetation. As reported by Bai et al. (2012), when plant residues enter the soils, their $\delta^{13}\text{C}$ values
344 may be modified slightly from their original values by isotope fractionation associated to preferential
345 C mineralization. Furthermore, studies conducted by Colombo et al. (2020) on a nearby rock glacier
346 at ~2700 m a.s.l., indicated $\delta^{13}\text{C}$ values of surrounding vegetated soils (-24.5 ‰) very similar to those
347 of the Plateau, while the $\delta^{13}\text{C}$ signature of the active rock glacier soil, characterized by cold ground
348 thermal regimes, coarse debris cover, and extremely reduced plant cover, increased considerably (ca.
349 -18 ‰). Thus, the overall correspondence of the $\delta^{13}\text{C}$ signatures between present-day vegetated soils
350 and paleosols under periglacial features suggested a common origin of the soil organic carbon from
351 very similar alpine flora.

352

353 **5. Historical and paleoenvironmental setting**

354 In Fig. 6 we propose a conceptual model reporting a tentative paleoenvironmental reconstruction
355 of the Stolenberg Plateau. Despite uncertainties, we believe that it may facilitate the interpretation of
356 our data and also the generation (and testing) of the different hypotheses, as it includes and
357 coordinates the different evidence we collected.

358 The LGM (Fig. 6A1-B1) ended around 22,000-19,000 yr BP (Ivy-Ochs et al., 2006a; Gianotti et
359 al., 2015; Ivy-Ochs, 2015; Monegato et al. 2017), during which transection glaciers, flowing into
360 valley systems, characterized the Western European Alps (Kelly et al., 2004). The mean air
361 temperature was ~12 °C lower than present day in the European Alps (Peyron et al., 1998; Becker et
362 al., 2016) and the mean July air temperature was likely around -4/5 °C on the Plateau (cf. Renssen et
363 al., 2009; Samartin et al., 2012a,b; Heiri et al., 2015). Considering the lack of soil samples older than
364 ca. 22,000 yr and the inferred cold conditions during LGM, together with the strongly weathered,
365 autochthonous soil and stone materials, we can hypothesize the presence of a barren cryoturbated
366 surface or of a small cold-based “ice cap” covering the Plateau (Fig. 6A1-B1).

367 Our oldest ¹⁴C datings (P3-2, P3-3, P2-9, and P2-9bis) span from 22,000 to 17,000 yr BP, falling
368 exactly during a period of massive downwasting of transection glaciers (Early Lateglacial Ice Decay-
369 ELID) (e.g., Ravazzi, 2005; Ivy-Ochs et al., 2006a, 2008; Monegato et al., 2007; Reitner, 2007;
370 Wirsig et al., 2016). Glacial shrinking also occurred at high elevations (Dielfolder and Hetzel, 2014),
371 with some mountain peaks, around 2300-2600 m a.s.l., protruding out of the ice surface (Wirsig et
372 al., 2016). The ELID occurred on both sides of the Alps due to significant rise in air temperatures
373 (e.g., Huber et al., 2010; Schmidt et al., 2012; Samartin et al., 2012a,b). Assuming a pronounced
374 climate continentality (Jost-Stauffer et al., 2001; Ivy-Ochs et al., 2009), summer air temperatures
375 were likely similar to the ones inferred for the Bølling-Allerød interstadial (e.g., Schmidt et al., 1998,
376 2012; Huber et al., 2010; Samartin et al., 2012a,b). In addition, soil surface temperatures in alpine
377 environments during summer are generally 2-4 °C above the air temperatures (Scherrer and Körner,
378 2010), indicating that life conditions of alpine organisms growing on the soil surface can be strongly
379 decoupled from conditions in the free atmosphere, particularly on south oriented surfaces like the

Commented [F1]: South east?

380 Plateau (e.g., Scherrer and Körner, 2010). Our ancillary measurements confirmed that the mean 10
381 cm depth soil temperature during summer was ~3 °C warmer than air temperature on the Plateau
382 (vegetated patch GST2), while at slightly lower elevation soil temperatures was 1-3 °C warmer
383 (Supplementary material 2, Tab. S2). Therefore, the Stolenberg Plateau was likely ice-free since
384 ~22,000-21,000 yr BP, i.e. the (micro)climatic conditions were probably suitable for pedogenesis and
385 growth of some vegetation (Fig. 6A2,3-B2,3).

386 No radiocarbon ages were detected in our soils between ~17,000 yr BP and ~14,700 yr BP, which
387 was a period (Gschnitz stadial or Oldest Dryas; Walker et al., 1999; Ivy-Ochs et al., 2006b, 2008)
388 characterized by a decrease of both temperatures and precipitations, with values 8.5-10 °C and 25-50
389 % lower than the respective modern values (Ivy-Ochs et al., 2006a,b; Kerschner and Ivy-Ochs, 2008;
390 Ivy-Ochs, 2015). These cold climatic conditions allowed a readvance of mountain glaciers (Kerschner
391 et al., 2002; Ivy-Ochs et al., 2006a,b, 2008). Thus, it is possible to hypothesize that the environmental
392 conditions on the Plateau might not have been suitable to sustain a sufficient plant life to produce
393 enough detectable organic carbon, while they favored strong frost-action processes which led to the
394 activation of periglacial features (Goodfellow, 2007; Ballantyne, 2010) (Fig. 6A4-B4).

395 The age of the P3-5 sample, dated between 13,337 and 13,110 cal. yr BP, matched perfectly with
396 a warm period occurred between ~14,700 and 12,900 yr BP, corresponding to the Bølling-Allerød
397 interstadial (Rasmussen et al., 2006; Ivy-Ochs et al., 2008; Dielfolder and Hetzel, 2014). A strong
398 rise in the mean annual air temperatures was inferred (ca. 3 °C), with respect to the Oldest Dryas,
399 causing the melting of valley glaciers (e.g., Ravazzi, 2005; Vescovi et al., 2007; Dielfolder and
400 Hetzel, 2014). Other studies indicated even greater rises in temperature, ~3-4 °C (Larocque-Tobler et
401 al., 2010) and ~5 °C (Renssen and Isarin, 2001). The mean July temperature at the Plateau, during
402 this period, may have been higher than 3 °C (cf., Heiri and Millet, 2005; Samartin et al., 2012a,b;
403 Dielfolder and Hetzel, 2014). Thus, the summer climate could have been suitable again for
404 pedogenesis and plant life (Fig. 6A5-B5).

405 After the Bølling-Allerød, a general worsening of climate conditions occurred, leading to another
406 cold phase, the Younger Dryas, also called Egesen Stadial (Ivy-Ochs et al., 2006b, 2008), which
407 lasted until 11,700 yr BP. The summer temperatures were 3.5-4 °C lower, while precipitation was
408 reduced by 10 to 30% compared to modern values (Kerschner et al., 2000, Kerschner and Ivy-Ochs,
409 2008). Again, on the Plateau, no soil organic matter radiocarbon ages were detected from this cold
410 period, as the environmental conditions likely favored frost-action processes rather than pedogenesis,
411 probably leading to a new expansion of periglacial features (Fig 6A6-B6).

412 The ages of four soil samples (P1-1, P1-2, P2-7, and P2-8) span from 8,800 to 5,600 yr BP,
413 corresponding to the warm Holocene Climatic Optimum (HCO), occurred between 10,000 and 5,000
414 yr BP (Mercuri, 2004; Orbelli, 2011). In this period, a ~3-4 °C temperature increase was estimated
415 with respect to the Younger Dryas (e.g., Tinner and Kaltenrieder, 2005; Ilyashuk et al., 2009;
416 Larocque-Tobler et al., 2010; Samartin et al., 2012b). Glaciers were probably smaller than present
417 day during the height of the HCO (e.g., Ivy-Ochs et al., 2009; Orbelli, 2011; Grämiger et al., 2018;
418 Bohleber et al., 2020). Mean air temperature was up to 1-2 °C warmer with respect to the present-day
419 values in the European Alps (e.g., Grove, 1988; Nesje and Dahl, 1993; Antonioli et al., 2000; Ivy-
420 Ochs et al., 2009) and the inferred July temperature at the Plateau may have reached values around
421 6-7 °C (or even more) (cf. Ilyashuk et al., 2009; Samartin et al., 2012b), therefore above present-day
422 values (cf., Birks and Willis, 2008; Ilyashuk et al., 2009; Samartin et al., 2012b). This likely led to
423 conditions suitable for plant life (Fig. 6A7-B7).

424 The age of our youngest sample (P4), dated 4,405-4,090 yr BP, corresponded with a period of
425 climate stability or slight cooling encompassed between 5,000 and 4,000 yr BP, after which a strong
426 decrease in temperature was estimated (Heiri et al., 2015), which led to Alpine glacier expansion
427 from 3,300 yr BP (Ivy-Ochs et al., 2009). After 3,300 yr BP, colder climatic conditions caused
428 prolonged and frequent glacier advances, leading finally to the Little Ice Age (LIA, 1300-1850 A.D.)
429 (Ivy-Ochs et al., 2009). During this last and prolonged cold phase, no soil radiocarbon ages were
430 detected at the Plateau, apart from highly weathered plant fragments collected deep inside the rock

431 wedge. The frost action likely prevailed, causing the final expansion of the periglacial features and
432 the complete covering of the Plateau (Fig. 6A8-B8), while few plants could thrive without being able
433 to leave measurable amounts of organic matter in the soil horizons.

434

435 **6. Nunataks: yes or no?**

436 The nunatak theory hypothesizes that unglaciated reliefs in glacial and periglacial areas acted as a
437 refugium for isolated colonies of microorganisms, plants, and animals which survived the rigorous
438 condition of the last glacial times for a few thousand years (Fairbridge, 1968; Dahl, 1987). These
439 nunataks could have served as center for the recolonization of the later deglaciated landscape
440 (Fairbridge, 1968). However, clear evidence for in situ survival of alpine floras on nunataks in the
441 Alps during the last ice age are rather limited (e.g., Stehlik, 2002; Schönswetter et al., 2005; Carcaillet
442 and Blarquez, 2017; Carcaillet et al., 2018) and subjected to a heated debate (e.g., Gugerli and
443 Holderegger, 2001; Carcaillet and Blarquez, 2019; Finsinger et al., 2019). The existence and
444 identification of such refugia during glacial or interglacial stages has been a topic of active research
445 for decades (Hampe et al., 2013). The recolonization of the Alps would have started not only from
446 peripheral refugia, but also from areas within the ice sheet (Schönswetter et al., 2005), where isolated
447 nunataks could have been sources and targets as well of species immigration and establishment (Paus
448 et al., 2006). Indeed, barren substrate or saprolite (Goodfellow, 2007), exposed just after glacier
449 retreat (Fig. 6A2-B2), could become targets of autotrophic organisms (e.g., algae, mosses, lichens,
450 higher plants), starting the process of primary succession (Bardgett et al., 2007). Thus, nunataks may
451 have been indeed inhabited for several thousand years during the last glaciation (Gugerli and
452 Holderegger, 2001), before the surrounding lowlands became deglaciated and invaded by organisms
453 in the early Holocene. Remarkably, the Plateau location matched exactly with an area assumed to be
454 a potential refugia for the survival of high-elevation plants on ice-free mountain tops within the
455 strongly glaciated central parts of the Alps, particularly among the north of the Aosta Valley (NW-

456 Italy) and south Valais, and within the mountain ranges of Monte Rosa (Stehlik, 2002; Schönswetter
457 et al., 2005; Kosiński et al., 2019).

458 Based on the results reported here and the presence of strong geomorphological evidences (i.e.
459 periglacial features such as blockstreams/blockfields), as well as the overall specific morphology,
460 aspect and position, the Stolenberg Plateau is thought to represent a Lateglacial Alpine Nunatak, on
461 which specific pedoclimatic conditions could have been suitable for alpine plant life already since
462 22,000-21,000 yr BP. As sometimes observed at high elevation at present day (e.g. *Saxifraga*
463 *oppositifolia* growing at 4500 m a.s.l. near the summit of Dom in Switzerland, Körner, 2011, or many
464 other species up to ca. 4000 m a.s.l., Boucher et al., 2021), soil/substrate temperatures can be
465 increased by solar surface warming in specific protected sites. This is particularly true where adiabatic
466 winds, topography, local rock warming effect (Carturan et al., 2013), long-wave radiation from
467 nearby rocky walls (i.e., the Mt. Stolenberg rock wall), and mass elevation effect (e.g. Monte Rosa
468 Massif) (Samartin et al., 2012a), favor specific and stable microclimate features (e.g., Stewart and
469 Lister, 2001), allowing the formation of the nunatak conditions.

470

471 **6. Conclusion**

472 In the severe periglacial environment of the Stolenberg Plateau, at 3030 m a.s.l., thick and well-
473 developed Umbrisol were detected inside periglacial features (blockstreams/blockfields). As
474 previously reported in Pintaldi et al (2021), these soils showed carbon stocks comparable to alpine
475 tundra or even forest soils, despite the large stony cover and the scattered vegetation. Radiocarbon
476 dating and soil $\delta^{13}\text{C}$ signatures indicated that these hidden soils were paleosols that recorded
477 exclusively the main warming phases occurring since the end of LGM until the beginning of the Late
478 Holocene cooling. This finding suggests that the environmental conditions on the Plateau were
479 suitable for alpine plant life and pedogenesis, already since the end of LGM. Our results, coupled
480 with the inferred paleoclimate reconstruction, indicate that the Stolenberg Plateau can be considered

481 a direct evidence of a Lateglacial Alpine Nunatak, representing therefore a valuable natural and
482 historical archive for unravelling the post-LGM history of the high-elevation landscape of the
483 European Alps.

484

485 **Acknowledgments**

486 This study was supported by European Regional Development Fund in Interreg Alpine Space project
487 Links4Soils (ASP399): Caring for Soil-Where Our Roots Grow
488 (<http://www.alpinespace.eu/projects/links4soils/en/the-project>). Many thanks to Monterosa Ski
489 Resort (Monterosa 2000 and Monterosa SpA project stakeholders) for providing logistical support.

490

491 **References**

- 492 Antonioli, F., Baroni, C., Camuffo, D., et al., 2000. Le fluttuazioni del clima nel corso dell'Olocene:
493 stato dell'arte. *Il Quaternario* 13(1/2), 95–128.
- 494 Bai, E., Boutton, T.W., Liu, F., et al., 2012. Spatial variation of soil $\delta^{13}\text{C}$ and its relation to carbon
495 input and soil texture in a subtropical lowland woodland. *Soil Biol. Biochem.* 44(1), 102–112.
496 <https://doi.org/10.1016/j.soilbio.2011.09.013>
- 497 Ballantyne, C.K., 1998. Age and significance of mountain-top detritus. *Permafr. Periglac. Process.*
498 9, 327–345. [https://doi.org/10.1002/\(SICI\)1099-1530\(199810/12\)9:4<327::AID-
499 PPP298>3.0.CO;2-9](https://doi.org/10.1002/(SICI)1099-1530(199810/12)9:4<327::AID-PPP298>3.0.CO;2-9)
- 500 Ballantyne, C.K., 2010. A general model of autochthonous blockfield evolution. *Permafr. Periglac.*
501 *Process.* 21, 289–300. <https://doi.org/10.1002/ppp.700>
- 502 Ballantyne, C.K., Harris, C., 1994. *The Periglaciation of Great Britain*. Cambridge University Press,
503 Cambridge, U.K.
- 504 Bardgett, R.D., Richter, A., Bol, R., et al., 2007. Heterotrophic microbial communities use ancient
505 carbon following glacial retreat. *Biol. Lett.* 3, 487–490. <https://doi.org/10.1098/rsbl.2007.0242>

- 506 Baroni, C., Orombelli, G., 1996. The Alpine “Iceman” and Holocene Climatic Change. *Quat. Res.*
507 46, 78–83. <https://doi.org/10.1006/qres.1996.0046>
- 508 Becker, P., Seguinot, J., Juvet, G., et al., 2016. Last Glacial Maximum precipitation pattern in the
509 Alps inferred from glacier modelling. *Geogr. Helv.* 71, 173–187. [https://doi.org/10.5194/gh-](https://doi.org/10.5194/gh-71-173-2016)
510 71-173-2016
- 511 Berggren, G., 1969. Atlas of seeds and small fruits of Northwest-European plant species with
512 morphological descriptions. Part 2, Cyperaceae. Swedish Museum Natural History, Stockholm.
- 513 Berggren, G., 1981. Atlas of seeds and small fruits of Northwest-European plant species with
514 morphological descriptions. Part 3, Salicaceae-Cruciferae. Swedish Museum Natural History,
515 Stockholm.
- 516 Bertolotto, G., Martinetto, E., Vassio, E., 2012. Applicazioni paleobotaniche dello studio di resti
517 carpologici in suoli e depositi fluviali attuali del Piemonte, con particolare riferimento alle
518 Cyperaceae. *Inf. Bot. Ital.* 44 (2), 72–74.
- 519 Birks, H.H., 1994. Plant macrofossils and the nunatak theory of per-glacial survival. *Dissertationes*
520 *botanicae* 234, 129–143.
- 521 Birks, H.J.B., Willis, K.J., 2008. Alpines, trees, and refugia in Europe. *Plant Ecol. & Divers.* 1, 147–
522 160. <https://doi.org/10.1080/17550870802349146>
- 523 Bockheim, J.G., 2007. Importance of Cryoturbation in Redistributing Organic Carbon in Permafrost-
524 Affected Soils. *Soil Sci. Soc. Am. J.* 71, 1335. <https://doi.org/10.2136/sssaj2006.0414N>
- 525 Bockheim, J.G., Tarnocai, C., 1998. Recognition of cryoturbation for classifying permafrost-affected
526 soils. *Geoderma* 81, 281–293.
- 527 Bohleber, P., Schwikowski, M., Stocker-Waldhuber, M., et al., 2020. New glacier evidence for ice-
528 free summits during the life of the Tyrolean Iceman. *Scientific Rep.* 10(1), 1–10.
529 <https://doi.org/10.1038/s41598-020-77518-9>
- 530 Bojňanský, V., Fargašová, A., 2007. Atlas of Seeds and Fruits of Central and East-European Flora:
531 The Carpathian Mountains Region. Springer, Dordrecht, pp. 1046.

532 Boucher, F.C., Dentant, C., Ibanez, S., Capblanc, T., Boleda, M., Boulangeat, L., Smyčka, J., Roquet,
533 C., Lavergne, S., 2021. Discovery of cryptic plant diversity on the rooftops of the Alps. *Sci Rep*
534 11, 11128 (2021). <https://doi-org.inee.bib.cnrs.fr/10.1038/s41598-021-90612-w>

535 Calcagnile, L., Quarta, G., D'Elia, M., 2005. High-resolution accelerator-based mass spectrometry:
536 precision, accuracy and background. *Applied Radiation and Isotopes* 62(4), 623–629.
537 <https://doi.org/10.1016/j.apradiso.2004.08.047>

538 Carcaillet, C., 2001. Soil particles reworking evidences by AMS ¹⁴C dating of charcoal. *Comptes*
539 *Rendus de l'Académie des Sciences Paris, Série Earth and Planetary Sciences* 332, 21-28. DOI:
540 10.1016/S1251-8050(00)01485-3

541 Carcaillet, C., Blarquez, O., 2017. Fire ecology of a tree glacial refugium on a nunatak with a view
542 on Alpine glaciers. *New Phytol.* 216, 1281–1290. <https://doi.org/10.1111/nph.14721>

543 Carcaillet, C., Latil, J.-L., Abou, S., Ali, A., Ghaleb, B., Magnin, F., Roiron, P., and Aubert, S., 2018.
544 Keep your feet warm? A cryptic refugium of trees linked to a geothermal spring in an ocean of
545 glaciers, *Glob. Change Biol.*, 24, 2476–2487. <https://doi.org/10.1111/gcb.14067>

546 Carcaillet, C., Blarquez, O., 2019. Glacial refugia in the south-western Alps? *New Phytol.* 222(2),
547 663–667. <https://doi.org/10.1111/nph.15673>

548 Carraro, F., Giardino, M., 2004. Quaternary glaciations in the western Italian Alps - a review.
549 *Developments in Quaternary Science* 2(1), 201–208. [https://doi.org/10.1016/S1571-](https://doi.org/10.1016/S1571-0866(04)80071-X)
550 [0866\(04\)80071-X](https://doi.org/10.1016/S1571-0866(04)80071-X)

551 Carturan, L., Baroni, C., Becker, M., et al., 2013. Decay of a long-term monitored glacier: Careser
552 Glacier (Ortles-Cevedale, European Alps). *The Cryosphere* 7, 1819–1838.
553 <https://doi.org/10.5194/tc-7-1819-2013>, 2013.

554 Colombo, N., Ferronato, C., Antisari, L.V., et al., 2020. A rock-glacier–pond system (NW Italian
555 Alps): Soil and sediment properties, geochemistry, and trace-metal bioavailability. *Catena* 194,
556 104700. <https://doi.org/10.1016/j.catena.2020.104700>

557 Cossart, E., Fort, M., Bourles, D., et al., 2012. Deglaciation pattern during the Lateglacial/Holocene
558 transition in the southern French Alps. Chronological data and geographical reconstruction
559 from the Claree Valley (upper Durance catchment, southeastern France). *Palaeogeography*
560 *Palaeoclimatology Palaeoecology* 315-316: 109-123. doi:10.1016/j.palaeo.2011.11.017

561 D'Amico, M.E., Catoni, M., Terribile, F., et al., 2016. Contrasting environmental memories in relict
562 soils on different parent rocks in the south-western Italian Alps. *Quat. Int.* 418, 61–74.
563 <https://doi.org/10.1016/j.quaint.2015.10.061>

564 D'Amico, M.E., Pintaldi, E., Catoni, M., et al., 2019. Pleistocene periglacial imprinting on
565 polygenetic soils and paleosols in the SW Italian Alps. *Catena* 174, 269–284.
566 <https://doi.org/10.1016/j.catena.2018.11.019>

567 Dahl, E., 1987. The nunatak theory reconsidered. *Ecol. Bull.* 77–94.
568 <https://www.jstor.org/stable/20112974>

569 D'Elia, M., Calcagnile, L., Quarta, G., et al., 2004. Sample preparation and blank values at the AMS
570 radiocarbon facility of the University of Lecce. *Nuclear Instruments and Methods in Physics*
571 *Research Section B: Beam Interactions with Materials and Atoms* 223, 278–283.
572 <https://doi.org/10.1016/j.nimb.2004.04.056>

573 Deline, P., Orombelli, G., 2005. Glacier fluctuations in the western Alps during the Neoglacial, as
574 indicated by the Miage morainic amphitheatre (Mont Blanc massif, Italy). *Boreas* 34(4), 456–
575 467. <https://doi.org/10.1111/j.1502-3885.2005.tb01444.x>

576 Dielfolder, A., Hetzel, R., 2014. The deglaciation history of the Simplon region (southern Swiss Alps)
577 constrained by ¹⁰Be exposure dating of ice-molded bedrock surfaces. *Quat. Sci. Rev.* 84, 26–
578 38. <https://doi.org/10.1016/j.quascirev.2013.11.008>

579 Egli, M., Sartori, G., Mirabella, A., et al., 2009. Effect of north and south exposure on organic matter
580 in high Alpine soils. *Geoderma* 149(1-2), 124–136.
581 <https://doi.org/10.1016/j.geoderma.2008.11.027>

582 Eglinton, T.I., Eglinton, G., Dupont, L., et al., 2002. Composition, age, and provenance of organic
583 matter in NW African dust over the Atlantic Ocean. *Geochemistry, Geophysics, Geosystems*,
584 3(8), 1–27. <https://doi.org/10.1029/2001GC000269>

585 Ercole, E., Pistarino, A., Martinetto, E., et al., 2012. Atlante fotografico dei frutti e dei semi della
586 flora del Piemonte e della Valle d'Aosta: Cyperaceae: *Bollettino del Museo Regionale di*
587 *Scienze Naturali di Torino*, v. 29, no. 1, p. 5–34, 133–283

588 Fairbridge, R.W., 1968. Glacial refuges (nunatak theory). In: *Geomorphology. Encyclopedia of Earth*
589 *Science*. Springer, Berlin, Heidelberg.

590 Favilli, F., Egli, M., Cherubini, P., et al., 2008. Comparison of different methods of obtaining a
591 resilient organic matter fraction in Alpine soils. *Geoderma* 145, 355–369.
592 <https://doi.org/10.1016/j.geoderma.2008.04.002>

593 Favilli, F., Egli, M., Brandova, D., et al., 2009. Combined use of relative and absolute dating
594 techniques for detecting signals of Alpine landscape evolution during the late Pleistocene and
595 early Holocene. *Geomorphol.* 112, 48–66. <https://doi.org/10.1016/j.geomorph.2009.05.003>

596 Finsinger, W., Schwörer, C., Heiri, O., et al., 2019. Fire on ice and frozen trees? Inappropriate
597 radiocarbon dating leads to unrealistic reconstructions. *New Phytol.* 222, 657–662.
598 <https://doi.org/10.1111/nph.15354>

599 Freppaz, M., Viglietti D., Balestrini, R., et al., 2019. Climatic and pedoclimatic factors driving C and
600 N dynamics in soil and surface water in the alpine tundra (NW-Italian Alps). *Nat Conserv* 34,
601 67–90. <https://doi.org/10.3897/natureconservation.34.30737>

602 Gianotti, F., Forno, M.G., Ivy-Ochs, S., et al., 2015. Stratigraphy of the Ivrea morainic amphitheatre
603 (NW Italy) an updated synthesis. *Alp. Medit. Quat.* 28, 29–58. ISSN: 2279-733

604 Goodfellow, B., 2007. Relict non-glacial surfaces in formerly glaciated landscapes. *Earth-Sci. Rev.*
605 80, 47–73. <https://doi.org/10.1016/j.earscirev.2006.08.002>

606 Grämiger, L.M., Moore, J.R., Gischig, V.S., et al., 2018. Thermomechanical stresses drive damage
607 of Alpine valley rock walls during repeat glacial cycles. *J. Geophys. Res.: Earth Surface*
608 123(10), 2620–2646. <https://doi.org/10.1029/2018JF004626>

609 Graven, H.D., 2015. Impact of fossil fuel emissions on atmospheric radiocarbon and various
610 applications of radiocarbon over this century. *Proc. Nat. Academy Sci.* 112(31), 9542–9545.
611 <https://doi.org/10.1073/pnas.1504467112>

612 Grove, J.M., 1988. *The Little Ice Age*. Methuen, London, pp. 498.

613 Gugerli, F., Holderegger, R., 2001. Nunatak survival, tabula rasa and the influence of the Pleistocene
614 ice-ages on plant evolution in mountain areas. *Trends in Plant Science* 6, 397–398.
615 [https://doi.org/10.1016/S1360-1385\(01\)02053-2](https://doi.org/10.1016/S1360-1385(01)02053-2)

616 Hampe, A., Rodríguez-Sánchez, F., Dobrowski, S., et al., 2013. Climate refugia: from the Last Glacial
617 Maximum to the twenty-first century. *New Phytol.* 197, 16–18.
618 <https://doi.org/10.1111/nph.12059>

619 Hatté, C., Pessenda, L.C., Lang, A., et al., 2001. Development of accurate and reliable ¹⁴C
620 chronologies for loess deposits: application to the loess sequence of Nussloch (Rhine valley,
621 Germany). *Radiocarbon* 43(2B), 611–618. <https://doi.org/10.1017/S0033822200041266>

622 Hättestrand, C., Stroeven, A.P., 2002. A relict landscape in the centre of Fennoscandian glaciation;
623 geomorphological evidence of minimal Quaternary glacial erosion. *Geomorphology* 44(1–2),
624 127–143. [https://doi.org/10.1016/S0169-555X\(01\)00149-0](https://doi.org/10.1016/S0169-555X(01)00149-0)

625 Heiri, O., Koinig, K.A., Spötl, C., et al., 2014. Palaeoclimate records 60–8 ka in the Austrian and
626 Swiss Alps and their forelands. *Quaternary Science Reviews*, 106, 186–
627 205. <https://doi.org/10.1016/j.quascirev.2014.05.021>

628 Heiri, O., Ilyashuk, B., Millet, L., et al., 2015. Stacking of discontinuous regional palaeoclimate
629 records: Chironomid-based summer temperatures from the Alpine region. *The Holocene* 25,
630 137–149. <https://doi.org/10.1177/0959683614556382>

631 Heiri, O., Millet, L., 2005. Reconstruction of Late Glacial summer temperatures from chironomid
632 assemblages in Lac Lautrey (Jura, France). *J. Quat. Sci.* 20, 33–44.
633 <https://doi.org/10.1002/jqs.895>

634 Hoffmann, H.M., 2016. Micro radiocarbon dating of the particulate organic carbon fraction in Alpine
635 glacier ice: method refinement, critical evaluation and dating applications [PhD dissertation].
636 Combined Faculties for the Natural Sciences and for Mathematics of the Ruperto-Carola
637 University of Heidelberg. <https://doi.org/10.11588/heidok.00020712>

638 Hormes, A., Karlén, W., Possnert, G., 2004. Radiocarbon dating of palaeosol components in moraines
639 in Lapland, northern Sweden. *Quat. Sci. Rev.* 23(18-19), 2031–2043.
640 <https://doi.org/10.1016/j.quascirev.2004.02.004>

641 Huber, K., Weckström, K., Drescher-Schneider, R., et al., 2010. Climate changes during the last
642 glacial termination inferred from diatom-based temperatures and pollen in a sediment core from
643 Längsee (Austria). *J. Paleolimnol.* 43, 131–147. <https://doi.org/10.1007/s10933-009-9322-y>

644 Ilyashuk, B.P., Gobet, E., Heiri, O., et al., 2009. Lateglacial environmental and climatic changes at
645 the Maloja Pass, Central Swiss Alps, as recorded by chironomids and pollen. *Quaternary*
646 *Science Reviews* 28(13-14), 1340–1353. <https://doi.org/10.1016/j.quascirev.2009.01.007>

647 IUSS Working Group WRB, 2015. World Reference Base for Soil Resources 2014, update 2015.
648 International soil classification system for naming soils and creating legends for soil maps.
649 World Soil Resources, Reports No. 106, FAO, Rome. E-ISBN 978-92-5-108370-3

650 Ivy-Ochs, S., 2015. Glacier variations in the European Alps at the end of the last glaciation.
651 *Cuadernos de Investigación Geográfica* 41, 295. <https://doi.org/10.18172/cig.2750>

652 Ivy-Ochs, S., Kerschner, H., Reuther, A., et al., 2006a. The timing of glacier advances in the northern
653 European Alps based on surface exposure dating with cosmogenic ^{10}Be , ^{26}Al , ^{36}Cl , and ^{21}Ne ,
654 in: *In Situ-Produced Cosmogenic Nuclides and Quantification of Geological Processes*.
655 Geological Society of America. [https://doi.org/10.1130/2006.2415\(04\)](https://doi.org/10.1130/2006.2415(04))

656 Ivy-Ochs, S., Kerschner, H., Kubik, P.W., et al., 2006b. Glacier response in the European Alps to
657 Heinrich Event 1 cooling: the Gschnitz stadial. *J. Quat. Sci.* 21, 115–130.
658 <https://doi.org/10.1002/jqs.955>

659 Ivy-Ochs, S., Kerschner, H., Reuther, A., et al., 2008. Chronology of the last glacial cycle in the
660 European Alps. *J. Quat. Sci.* 23, 559–573. <https://doi.org/10.1002/jqs.1202>

661 Ivy-Ochs, S., Kerschner, H., Maisch, M., et al., 2009. Latest Pleistocene and Holocene glacier
662 variations in the European Alps. *Quat. Sci. Rev.* 28, 2137–2149.
663 <https://doi.org/10.1016/j.quascirev.2009.03.009>

664 Ivy-Ochs, S., Kober, F., 2013. COSMOGENIC NUCLIDE DATING | Exposure Geochronology, in:
665 *Encyclopedia of Quaternary Science*. Elsevier, 432–439. <https://doi.org/10.1016/B978-0-444-53643-3.00034-0>

666

667 Jenk, T.M., Szidat, S., Bolius, D., et al., 2009. A novel radiocarbon dating technique applied to an ice
668 core from the Alps indicating late Pleistocene ages. *J. Geophys. Res.* 114, D14305.
669 <https://doi.org/10.1029/2009JD011860>

670 Jenk, T.M., Szidat, S., Schwikowski, M., et al., 2006. Radiocarbon analysis in an Alpine ice core:
671 record of anthropogenic and biogenic contributions to carbonaceous aerosols in the past (1650-
672 1940). *Atmos. Chem. Phys.* 6, 5381–5390. <https://doi.org/10.5194/acp-6-5381-2006>

673 Jost-Stauffer, M., Coope, G.R., Schlüchter, C., 2001. A coleopteran fauna from the middle Würm
674 (Weichselian) of Switzerland and its bearing on palaeobiogeography, palaeoclimate and
675 palaeoecology. *J. Quat. Sci.* 16, 257–268. <https://doi.org/10.1002/jqs.616>

676 Karte, J., 1983. Periglacial Phenomena and their Significance as Climatic and Edaphic Indicators.
677 *GeoJournal* 7, 329–340.

678 Kelly, M.A., Buoncristiani, J.-F., Schlochter, C., 2004. A reconstruction of the last glacial maximum
679 (LGM) ice-surface geometry in the western Swiss Alps and contiguous Alpine regions in Italy
680 and France. *Eclogae Geol. Helv.* 97, 57–75. <https://doi.org/10.1007/s00015-004-1109-6>

- 681 Kerschner, H., Ivy-Ochs, S., Schlüchter, C., 2002. Die Moräne von Trins im Gschnitztal. *Innsbrucker*
682 *Geographische Studien* 33(2), 185–194.
- 683 Kerschner, H., Ivy-Ochs, S., 2008. Palaeoclimate from glaciers: Examples from the Eastern Alps
684 during the Alpine Lateglacial and early Holocene. *Global Planet. Change* 60, 58–71.
685 <https://doi.org/10.1016/j.gloplacha.2006.07.034>
- 686 Kerschner, H., Kaser, G., Sailer, R., 2000. Alpine Younger Dryas glaciers as palaeo-precipitation
687 gauges. *Ann. Glaciol.* 31, 80–84. <https://doi.org/10.3189/172756400781820237>
- 688 Kleman, J., Borgström, I., 1990. The boulder fields of Mt. Fulufjället, west-central Sweden.
689 *Geografiska Annaler* 72A (1), 63–78. <https://doi.org/10.2307/521238>
- 690 Köhler, P., 2016. Using the Suess effect on the stable carbon isotope to distinguish the future from
691 the past in radiocarbon. *Environ. Res. Lett.* 11(12), 124016.
692 <https://iopscience.iop.org/article/10.1088/1748-9326/11/12/124016>
- 693 Körner, C., 2003. *Alpine Plant Life*. Springer Berlin Heidelberg, Berlin, Heidelberg.
694 <https://doi.org/10.1007/978-3-642-18970-8>
- 695 Körner, C., 2011. Coldest places on Earth with angiosperm plant life. *Alp. Bot.* 121, 11–22.
696 <https://doi.org/10.1007/s00035-011-0089-1>
- 697 Körner, C., Leuzinger, S., Riedl, S., et al., 2016. Carbon and nitrogen stable isotope signals for an
698 entire alpine flora, based on herbarium samples. *Alp. Bot.* 126(2), 153–166.
699 <https://doi.org/10.1007/s00035-016-0170-x>
- 700 Kosiński, P., Sękiewicz, K., Walas, Ł., et al., 2019. Spatial genetic structure of the endemic alpine
701 plant *Salix serpyllifolia*: genetic swamping on nunataks due to secondary colonization? *Alp.*
702 *Bot.* 129(2), 107–121. <https://doi.org/10.1007/s00035-019-00224-4>
- 703 Kullman, L., 2008. Early postglacial appearance of tree species in Northern Scandinavia: review and
704 perspective. *Quat. Sci. Rev.* 27(27-28), 2467–2472.
705 <https://doi.org/10.1016/j.quascirev.2008.09.004>

- 706 Lang, G., 1994. Quartäre Vegetationsgeschichte Europas: Methoden und Ergebnisse. G. Fischer,
707 Schaffhausen.
- 708 Larocque-Tobler, I., Heiri, O., Wehrli, M., 2010. Late Glacial and Holocene temperature changes at
709 Egelsee, Switzerland, reconstructed using subfossil chironomids. *J. Paleolimnol.* 43, 649–666.
710 <https://doi.org/10.1007/s10933-009-9358-z>
711
- 712 Lowe, J.J., Walker, M.J., 2000. Radiocarbon Dating the Last Glacial-Interglacial Transition (Ca. 14–
713 9 ¹⁴C Ka Bp) in Terrestrial and Marine Records: The Need for New Quality Assurance
714 Protocols 1. *Radiocarbon* 42(1), 53–68. <https://doi.org/10.1017/S0033822200053054>
- 715 Magnani, A., Viglietti, D., Godone, D., et al., 2017. Interannual Variability of Soil N and C Forms in
716 Response to Snow-Cover duration and Pedoclimatic Conditions in Alpine Tundra, Northwest
717 Italy. *Arct Antarct Alp Res* 49, 227–242. <https://doi.org/10.1657/AAAR0016-037>
- 718 Martinetto, E., Vassio, E., 2010. Reconstructing “Plant Community Scenarios” by means of
719 palaeocarpological data from the CENOFITA database, with an example from the Ca' Viettone
720 site (Pliocene, Northern Italy). *Quat. Int.* 225(1), 25–36.
721 <https://doi.org/10.1016/j.quaint.2009.08.020>
- 722 McCarroll, D., Ballantyne, C.K., Nesje, A., et al., 1995. Nunataks of the last ice sheet in northwest
723 Scotland. *Boreas* 24, 305–323. <https://doi.org/10.1111/j.1502-3885.1995.tb00782.x>
- 724 Mercalli, L., 2004. Il clima terrestre negli ultimi 10'000 anni. <https://doi.org/10.5169/seals-132929>
- 725 Monegato, G., Ravazzi, C., Donegana, M., et al., 2007. Evidence of a two-fold glacial advance during
726 the last glacial maximum in the Tagliamento end moraine system (eastern Alps). *Quat. Res.* 68,
727 284–302. <https://doi.org/10.1016/j.yqres.2007.07.002>
- 728 Monegato, G., Scardia, G., Hajdas, I., et al., 2017. The Alpine LGM in the boreal ice-sheets game.
729 *Scientific Reports*, 7(1), 1-8. <https://doi.org/10.1038/s41598-017-02148-7>
- 730 Muhs, D.R., Ager, T.A., Bettis, E.A., et al., 2003. Stratigraphy and palaeoclimatic significance of
731 Late Quaternary loess-palaeosol sequences of the Last Interglacial-Glacial cycle in central

732 Alaska. *Quat Sci Rev*, 22(18–19): 1947–1986. [https://doi.org/10.1016/S0277-3791\(03\)00167-](https://doi.org/10.1016/S0277-3791(03)00167-7)
733 7

734 Nesje, A., Dahl, S.O., Anda, E., et al., 1988. Block fields in southern Norway: significance for the
735 Late Weichselian ice sheet. *Norsk Geologisk Tidsskrift* 68, 149–169.

736 Nesje, A., Dahl, S.O., 1993. Lateglacial and Holocene glacier fluctuations and climate variations in
737 western Norway: a review. *Quat. Sci. Rev.* 12, 255–261. [https://doi.org/10.1016/0277-](https://doi.org/10.1016/0277-3791(93)90081-V)
738 3791(93)90081-V

739 Orombelli, G., 1998. Le torbe del Rutor: una successione significativa per la storia olocenica dei
740 ghiacciai e del clima nelle Alpi. *Memorie della Società Geografica Italiana* 55, 153–165.

741 Orombelli, G., 2011. Holocene mountain glacier fluctuations: a global overview. *Geografia Fisica e*
742 *Dinamica Quaternaria* 34(1), 17–24.

743 Orombelli, G., Ravazzi, C., Cita, M.B., 2005. Osservazioni sul significato dei termini LGM (UMG),
744 Tardoglaciale e postglaciale in ambito globale, italiano ed alpino. *Il Quaternario* 18(2), 147–
745 156.

746 Paus, A., Velle, G., Larsen, J., et al., 2006. Lateglacial nunataks in central Scandinavia:
747 Biostratigraphical evidence for ice thickness from Lake Flåfattjønn, Tynset, Norway. *Quat. Sci.*
748 *Rev.* 25, 1228–1246. <https://doi.org/10.1016/j.quascirev.2005.10.008>

749 Pessenda, L. C., Gouveia, S. E., Aravena, R., 2001. Radiocarbon dating of total soil organic matter
750 and humin fraction and its comparison with ¹⁴C ages of fossil charcoal. *Radiocarbon* 43(2B),
751 595–601. <https://doi.org/10.1017/S0033822200041242>

752 Peyron, O., Guiot, J., Cheddadi, R., et al., 1998. Climatic reconstruction in Europe for 18,000 yr BP
753 from pollen data. *Quat. Res.* 49, 183–196. <https://doi.org/10.1006/qres.1997.1961>

754 Pintaldi, E., D'Amico, M.E., Colombo, N., et al., 2021. Hidden soils and their carbon stocks at high-
755 elevation in the European Alps (North-West Italy). *Catena* 198, 105044.
756 <https://doi.org/10.1016/j.catena.2020.105044>

757 Pintaldi, E., D'Amico, M.E., Siniscalco, C., et al., 2016. Hummocks affect soil properties and soil-
758 vegetation relationships in a subalpine grassland (North-Western Italian Alps). *Catena* 145,
759 214–226. <https://doi.org/10.1016/j.catena.2016.06.014>

760 Rasmussen, S.O., Andersen, K.K., Svensson, A.M., et al., 2006. A new Greenland ice core
761 chronology for the last glacial termination. *J. Geophys. Res.* 111, D06102.
762 <https://doi.org/10.1029/2005JD006079>

763 Ravazzi, C., 2005. Il Tardoglaciale: suddivisione stratigrafica, evoluzione sedimentaria e
764 vegetazionale nelle Alpi e in Pianura Padana. *Studi Trent. Sci. Nat., Acta Geol* 82, 17–29.

765 Reimer, P. J., Austin, W. E., Bard, E., Bayliss, A., Blackwell, P. G., Ramsey, C. B., ... & Talamo, S.,
766 2020. The IntCal20 Northern Hemisphere radiocarbon age calibration curve (0–55 cal kBP).
767 *Radiocarbon*, 62(4), 725–757. <https://doi.org/10.1017/RDC.2020.41>

768 Reitner, J.M., 2007. Glacial dynamics at the beginning of Termination I in the Eastern Alps and their
769 stratigraphic implications. *Quat. Int.* 164–165, 64–84.
770 <https://doi.org/10.1016/j.quaint.2006.12.016>

771 Renssen, H., Isarin, R.F.B., 2001. The two major warming phases of the last deglaciation at 14.7 and
772 11.5 ka cal BP in Europe: climate reconstructions and AGCM experiments. *Global and*
773 *Planetary Change* 30, 117–153.

774 Renssen, H., Seppä, H., Heiri, O., et al., 2009. The spatial and temporal complexity of the Holocene
775 thermal maximum. *Nature Geoscience*, 2(6), 411–414. <https://doi.org/10.1038/ngeo513>

776 Ruellan, A., 1971. The history of soils: some problems of definition and interpretation. In: Yaalon,
777 D.H. (Ed.), *Paleopedology: Origin, Nature and Dating of Paleosols*. International Society of
778 Soil Science and Israel Universities Press, Jerusalem, Israel, pp. 3–13.

779 Rumpel, C., Kögel-Knabner, I., Bruhn, F., 2002. Vertical distribution, age and chemical composition
780 of organic carbon in two forest soils of different pedogenesis. *Org. Geochem.* 3, 1131–1142.
781 [https://doi.org/10.1016/S0146-6380\(02\)00088-8](https://doi.org/10.1016/S0146-6380(02)00088-8)

782 Samartin, S., Heiri, O., Lotter, A. F., et al., 2012a. Climate warming and vegetation response after
783 Heinrich event 1 (16 700–16 000 cal yr BP) in Europe south of the Alps. *Climate of the Past*
784 8(6), 1913–1927. <https://doi.org/10.5194/cp-8-1913-2012>

785 Samartin, S., Heiri, O., Vescovi, E., et al., 2012b. Lateglacial and early Holocene summer
786 temperatures in the southern Swiss Alps reconstructed using fossil chironomids. *J. Quat. Sci.*
787 27, 279–289. <https://doi.org/10.1002/jqs.1542>

788 Sartori, G., Mancabelli, A., Corradini, F., et al., 2001. Verso un catalogo dei suoli del Trentino: 3.
789 Rendzina (Rendzic Leptosols) e suoli rendziniformi. *Studi Trentini Sci. Nat. Acta Geol.* 76, 43–
790 70.

791 Scharpenseel, H.W., Becker-Heidmann, P., 1992. Twenty-five years of radiocarbon dating soils:
792 paradigm of erring and learning. *Radiocarbon* 34, 541–549. doi:10.1017/S0033822200063803

793 Scherrer, D., Koerner, C., 2010. Infra-red thermometry of alpine landscapes challenges climatic
794 warming projections. *Global Change Biology* 16(9), 2602–2613.
795 <https://doi.org/10.1111/j.1365-2486.2009.02122.x>

796 Schmidt, R., Wunsam, S., Brosch, U., et al., 1998. Late and post-glacial history of meromictic
797 Längsee (Austria), in respect to climate change and anthropogenic impact. *Aquat. Sci.* 60, 56–
798 88

799 Schmidt, R., Weckström, K., Lauterbach, S., et al., 2012. North Atlantic climate impact on early late-
800 glacial climate oscillations in the south-eastern Alps inferred from a multi-proxy lake sediment
801 record. *J. Quat. Sci.* 27, 40–50. <https://doi.org/10.1002/jqs.1505>

802 Schönswetter, P., Stehlik, I., Holderegger, R., et al., 2005. Molecular evidence for glacial refugia of
803 mountain plants in the European Alps. *Mol. Ecol.* 14, 3547–3555.
804 <https://doi.org/10.1111/j.1365-294X.2005.02683.x>

805 Serra, E., Valla, P.G., Gribenski, N., et al., 2021. Geomorphic response to the Lateglacial–Holocene
806 transition in high Alpine regions (Sanetsch Pass, Swiss Alps). *Boreas* 50(1), 242–261.
807 <https://doi-org./10.1111/bor.12480>

808 Smalley, I.J., Mavlyanova, N.G., Rakhmatullaev, K.L., et al., 2006. The formation of loess deposits
809 in the Tashkent region and parts of Central Asia; and problems with irrigation, hydrocollapse
810 and soil erosion. *Quat. Int.* 152, 59–69. <https://doi.org/10.1016/j.quaint.2005.12.002>

811 Stehlik, I., Blattner, F.R., Holderegger, R., et al., 2002. Nunatak survival of the high Alpine plant
812 *Eritrichium nanum* (L.) Gaudin in the central Alps during the ice ages. *Mol. Ecol.* 11, 2027–
813 2036. <https://doi.org/10.1046/j.1365-294X.2002.01595.x>

814 Stewart, J. R., Lister, A. M., 2001. Cryptic northern refugia and the origins of the modern biota.
815 *Trends in Ecology & Evolution* 16(11), 608–613. [https://doi.org/10.1016/S0169-](https://doi.org/10.1016/S0169-5347(01)02338-2)
816 [5347\(01\)02338-2](https://doi.org/10.1016/S0169-5347(01)02338-2)

817 Suess, H., 1955. Radiocarbon Concentration in Modern Wood. *Science* 122(3166), 415–417.
818 <http://www.jstor.org/stable/1751568>

819 Ter Heerdt, G.N.J., Verweij, G.L., Bekker, R.M., et al., 1996. An improved method for seed-bank
820 analysis: seedling emergence after removing the soil by sieving. *Funct. Ecol.* 10, 144–151.
821 <https://www.jstor.org/stable/2390273>

822 Thevenon, F., Anselmetti, F.S., Bernasconi, S.M., et al., 2009. Mineral dust and elemental black
823 carbon records from an Alpine ice core (Colle Gnifetti glacier) over the last millennium. *J.*
824 *Geophys. Res.* 114, D17102. <https://doi.org/10.1029/2008JD011490>

825 Thorn, C.E., Darmody, R.G., Holmqvist, J., et al., 2009. Comparison of radiocarbon dating of buried
826 paleosols using arbuscular mycorrhizae spores and bulk soil samples. *The Holocene*, 19(7),
827 1031-1037. <https://doi-org./10.1177/0959683609340997>

828 Tinner, W., Kaltenrieder, P., 2005. Rapid responses of high-mountain vegetation to early Holocene
829 environmental changes in the Swiss Alps. *J. Ecol.* 93(5), 936–947.
830 <https://www.jstor.org/stable/3599520>

831 Tognetto, F., Perotti, L., Viani, C., et al., 2021. Geomorphology and geosystem services of the Indren-
832 Cimalegna area (Monte Rosa massif – Western Italian Alps). *Journal of Maps* 17(2), 161–172.
833 DOI:10.1080/17445647.2021.1898484

834 Tonnejck, F.H., van der Plicht, J., Jansen, B., et al., 2006. Radiocarbon dating of soil organic matter
835 fractions in Andosols in northern Ecuador. *Radiocarbon* 48(3), 337–353.
836 <https://doi.org/10.1017/S0033822200038790>

837 van Vliet-Lanoë, B. 1998. Pattern ground, hummocks, and Holocene climatic changes. *Eurasian Soil*
838 *Sci.* 31, 507–513.

839 Vescovi, E., Ravazzi, C., Arpenti, E., et al., 2007. Interactions between climate and vegetation during
840 the Lateglacial period as recorded by lake and mire sediment archives in Northern Italy and
841 Southern Switzerland. *Quat. Sci. Rev.* 26, 1650–1669.
842 <https://doi.org/10.1016/j.quascirev.2007.03.005>

843 Velichkevich, F.Y., Zastawniak, E., 2006. Atlas of the Pleistocene Vascular Plant Macrofossils of
844 Central and Eastern Europe. Part I: Pteridophytes and Monocotyledons: W. Szafer Institute of
845 Botany, Polish Academy of Sciences, Krakow, pp. 224.

846 Velichkevich, F.Y., and Zastawniak, E., 2009. Atlas of the Pleistocene Vascular Plant Macrofossils
847 of Central and Eastern Europe. Part 2: Herbaceous Dicotyledons: W. Szafer Institute of Botany,
848 Polish Academy of Sciences, Krakow, pp. 380.

849 Wagenbach, D., Geis, K., 1989. The mineral dust record in a high altitude Alpine glacier (Colle
850 Gnifetti, Swiss Alps). In *Paleoclimatology and paleometeorology: modern and past patterns of*
851 *global atmospheric transport* (pp. 543-564). Springer, Dordrecht.

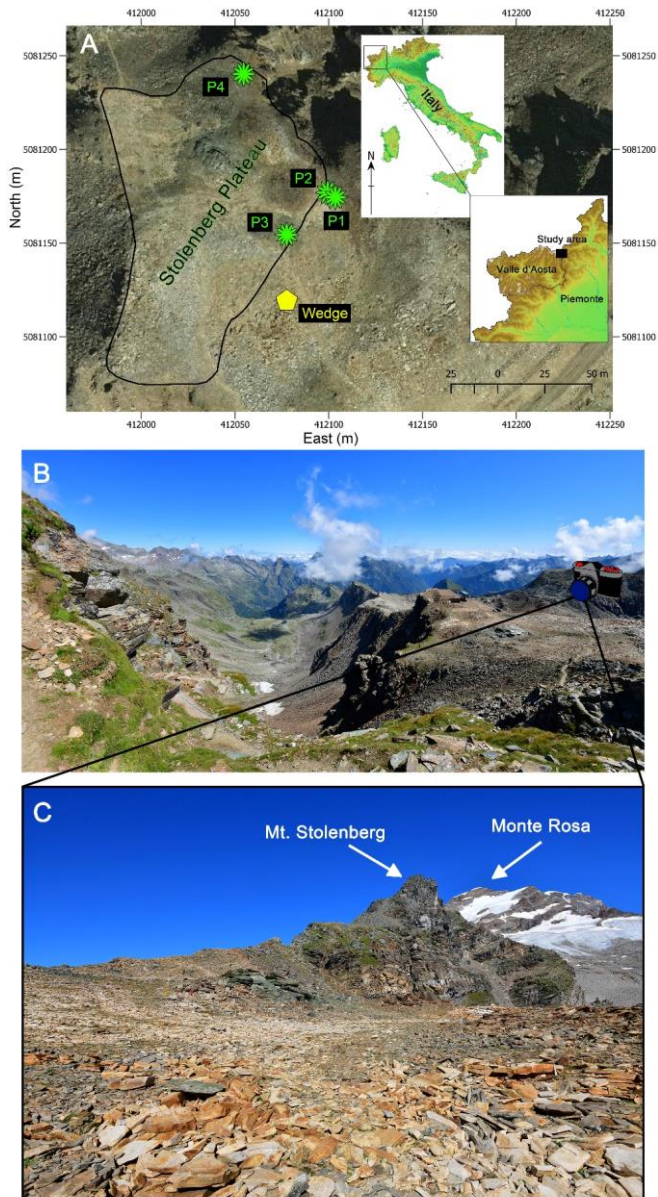
852 Wagenbach D., Preunkert S., Schäfer J., et al., 1996. Northward Transport of Saharan Dust Recorded
853 in a Deep Alpine Ice Core. In: Guerzoni S., Chester R. (eds) *The Impact of Desert Dust Across*
854 *the Mediterranean*. Environmental Science and Technology Library, vol 11. Springer,
855 Dordrecht.

856 Walker, M.J., Björck, S., Lowe, J.J., et al., 1999. Isotopic ‘events’ in the GRIP ice core: a stratotype
857 for the Late Pleistocene. *Quat. Sci. Rev.* 18, 1143–1150.

858 Walker, M. J., Berkelhammer, M., Björck, S., Cwynar, L. C., Fisher, D. A., Long, A. J., ... & Weiss,
859 H., 2012. Formal subdivision of the Holocene Series/Epoch: a Discussion Paper by a Working
860 Group of INTIMATE (Integration of ice-core, marine and terrestrial records) and the

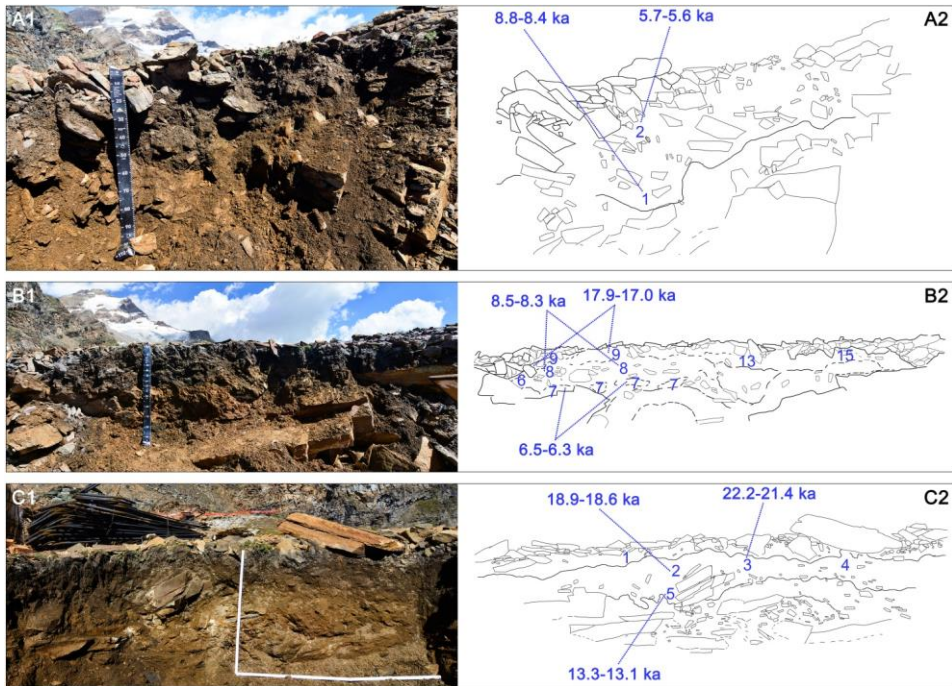
861 Subcommission on Quaternary Stratigraphy (International Commission on Stratigraphy).
862 Journal of Quaternary Science, 27(7), 649-659. Wang, Y., Amundson, R., Trumbore, S., 1996.
863 Radiocarbon dating of soil organic matter. Quaternary Research 45(3), 282–288.
864 <https://doi.org/10.1006/qres.1996.0029>
865 Wang, Z., Zhao, H., Dong, G., et al., 2014. Reliability of radiocarbon dating on various fractions of
866 loess-soil sequence for Dadiwan section in the western Chinese Loess Plateau. Frontiers of
867 Earth Science 8(4), 540–546. DOI 10.1007/s11707-014-0431-1
868 Wilson, P., 2013. Block/rock streams. The Encyclopedia of Quaternary Science 3, 514–522.
869 <https://doi.org/10.1016/B978-0-444-53643-3.00102-3>
870 Wirsig, C., Zasadni, J., Christl, M., et al., 2016. Dating the onset of LGM ice surface lowering in the
871 High Alps. Quat. Sci. Rev. 143, 37–50. <https://doi.org/10.1016/j.quascirev.2016.05.001>

872 **Figures**



873
874 **Figure 1.** (a) Location of the study area in the NW Italian Alps (www.pcn.minambiente.it) and overview of the
875 study area (orthoimage Piemonte Region, year 2010) (coordinate system WGS 84 / UTM zone 32N); green forms
876 indicate the location of the three soil profiles (P1, P2, P3) and the vegetated patch (P4); yellow polygon indicates

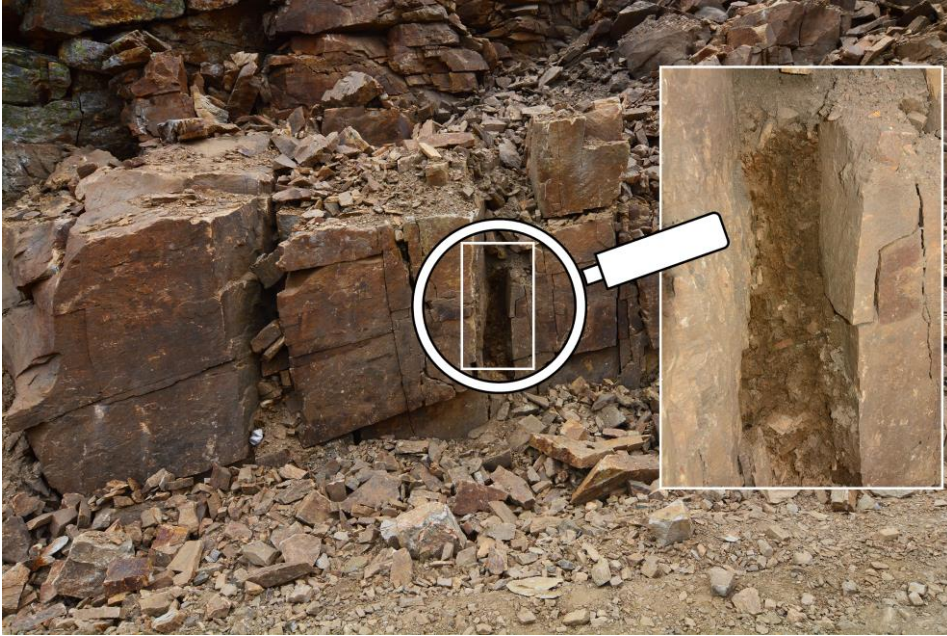
877 the location of the soil-filled wedge. (b) View of the Plateau from the base of the Mt. Stolenberg (photo by M.
878 D'Amico). (c) View of the Plateau (photo by M. D'Amico).



879
880
881
882
883
884
885
886
887

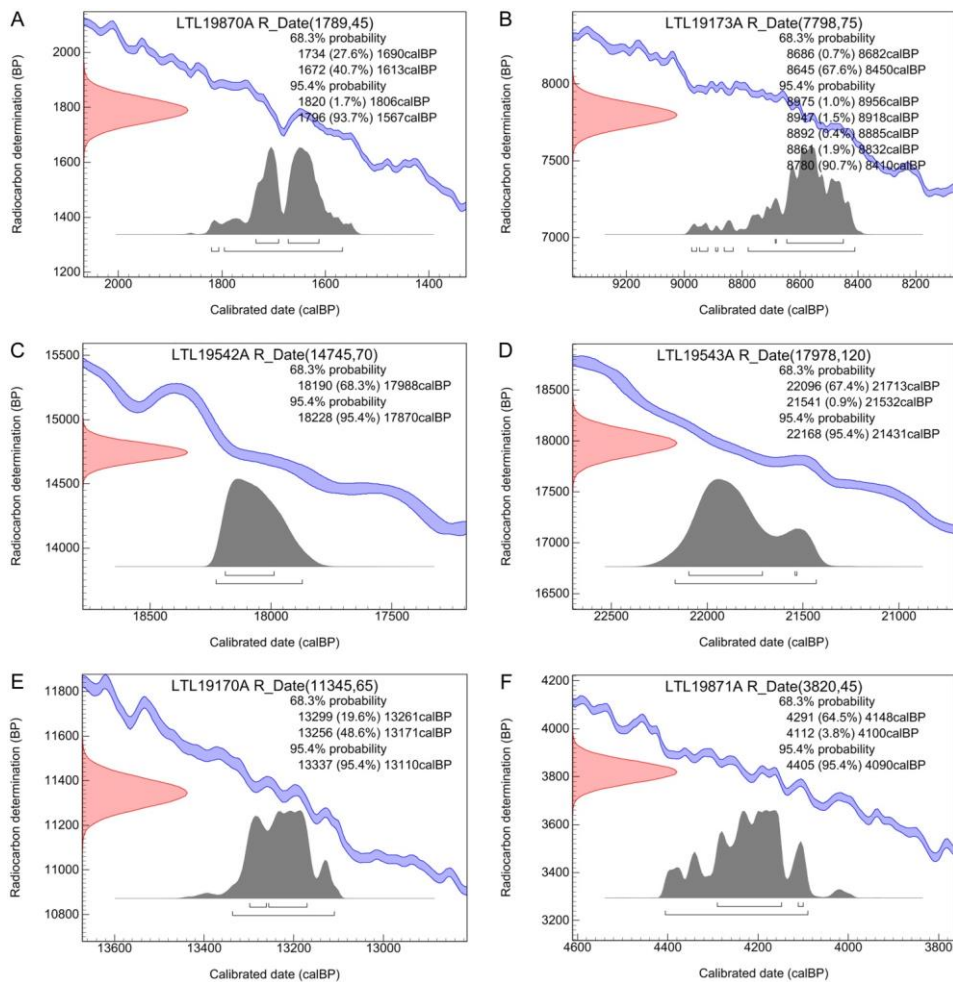
Figure 2. Soil profiles, with the corresponding scheme (on the side) reporting sampling points (number), the horizon limits (lines therein), and the age of soil samples (cal. ka BP). A1-A2: soil profile P1, samples P1-1 and P1-2 were analyzed for 14C (Tab. 2) and $\delta^{13}C$ (Tab. 3); B1-B2: soil profile P2, , samples P2-7, P2-8, and P2-9 (and P2-9bis, not shown in the figure) were analyzed for 14C (Tab. 2); P2-7, P2-8, P2-9 (and P2-9bis), P2-13, and P2-15 were analyzed for $\delta^{13}C$ (Tab. 3). C1-C2: soil profile P3, , samples P3-2, P3-3, and P3-5 were analyzed for 14C (Tab. 2); P3-1, P3-2, P3-3, P3-4, and P3-5 were analyzed for $\delta^{13}C$ (Tab. 3).

888
889

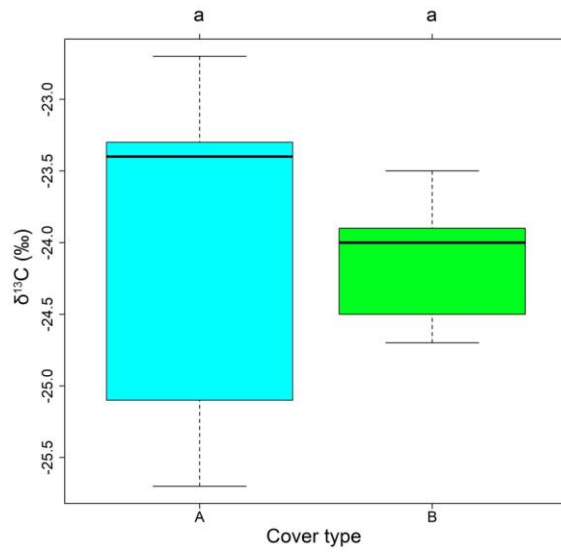


890
891
892
893

Figure 3. The soil-filled rock wedge along the southern border of the Plateau and detail of the sampling site.



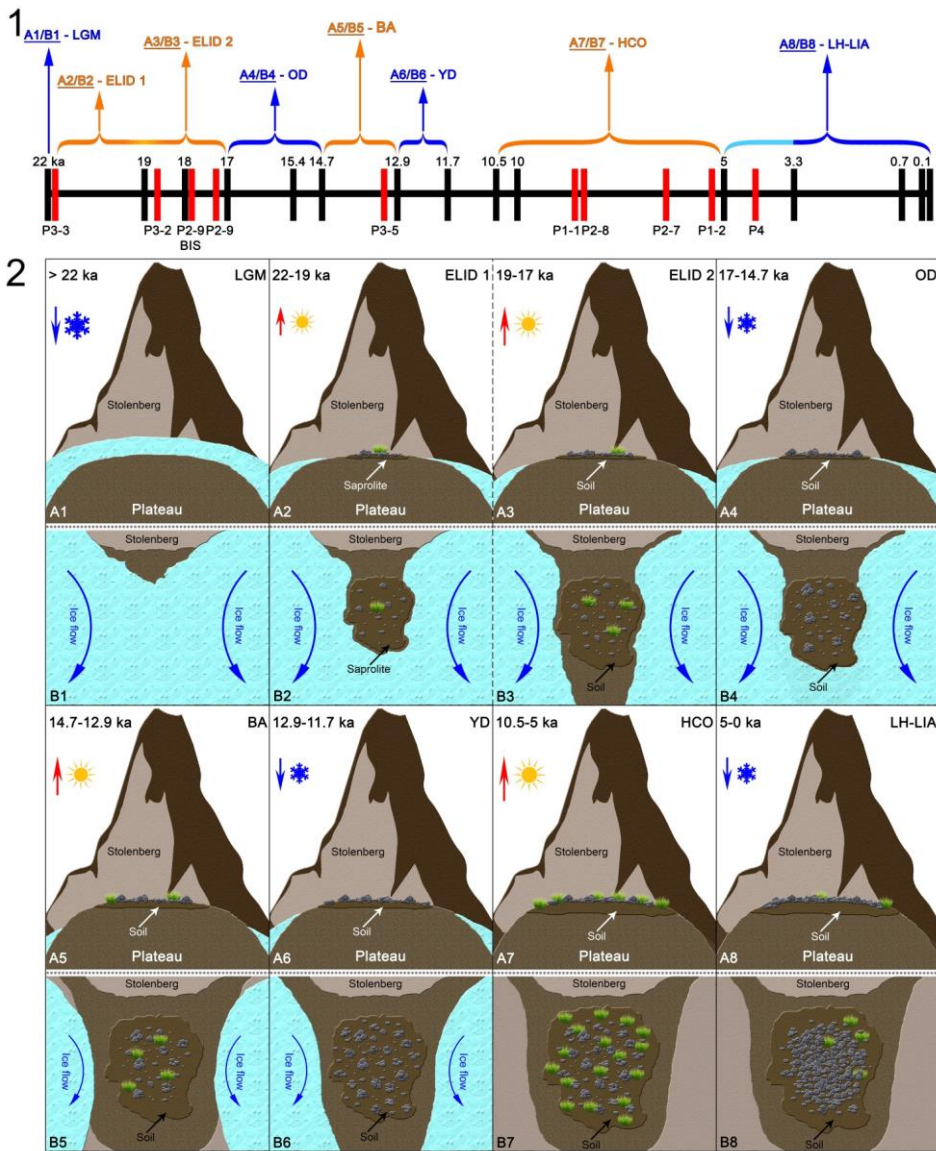
894
 895 **Figure 4. Radiocarbon date calibration of vegetation sample F (A) and soil samples P1-1 (B), P2-9bis (C); P3-3 (D),**
 896 **P3-5 (E), P4 (F). Radiocarbon date calibration of soil samples P1-2, P2-7,8,9 and P3-2 are reported in the**
 897 **Supplementary Material (Figs. S4-S8).**



898

899 **Figure 5. Boxplot (n=19) of $\delta^{13}\text{C}$ values of present-day vegetated soils (cover type A) and soils under**
900 **blockstream/blockfield (cover type B). Letters (a) on the top indicate the absence of statistically significant**
901 **differences among samples.**

902



903
 904
 905
 906
 907
 908
 909
 910
 911

Figure 6. Tentative paleoenvironmental reconstruction of the Stolenberg Plateau based on the findings in this paper and on literature reported in the text. LGM: Last Glacial Maximum; ELID: Early Lateglacial Ice Decay; OD: Oldest Dryas; BA: Bølling-Allerød; YD: Younger Dryas; HCO: Holocene Climatic Optimum; LH: Late Holocene; LIA Little Ice Age. (1) Reference timeline from LGM to present day: blue colors indicate cooling phases, orange ones warming phases, the light blue segment (on the right) indicates a period of progressive cooling occurred between HCO and the LH phase; red segments indicate the age of soil samples reported in table 2. (2) Corresponding visual of the Plateau during the different phases: letters A (A1, A2, etc.) are the frontal views, B ones are the planimetric views. Details in the text.

912
913

Tables

Profile samples		
Family/Genus/Species	N° (seeds/fruits/leaves)	Frequency (%)
Asteraceae indet.	1	0.3
Brassicaceae indet.	1	0.3
<i>Carex parviflora</i>	1	0.3
<i>Carex myosuroides</i>	7	1.9
<i>Cerastium</i> sp.	16	4.4
<i>Cerastium uniflorum</i>	90	24.6
<i>Cirsium</i> sp.	1	0.3
<i>Crepis</i> sp.	1	0.3
<i>Draba</i> sp.	1	0.3
<i>Gentiana</i> gr. <i>verna</i>	1	0.3
<i>Juncus</i> sp.	1	0.3
<i>Leucanthemopsis alpina</i>	1	0.3
<i>Minuartia</i> sp.	23	6.3
<i>Oxyria digyna</i>	1	0.3
Poaceae sp.	75	20.5
<i>Potentilla</i> sp.	1	0.3
<i>Salix</i> cf. <i>herbacea</i>	103	28.1
<i>Saxifraga oppositifolia</i>	10	2.7
<i>Sibbaldia procumbens</i>	1	0.3
<i>Silene acaulis</i>	27	7.4
<i>Taraxacum</i> cf. <i>alpinum</i>	2	0.5
cf. <i>Vaccinium uliginosum</i>	1	0.3
TOT	366	100.0
Wedge sample (F)		
Family/Genus/Species	N° (seeds/fruits/leaves)	Frequency (%)
cf. <i>Artemisia</i>	1	5.9
<i>Carex myosuroides</i>	1	5.9
<i>Cerastium</i> sp.	1	5.9
<i>Juncus</i> sp.	1	5.9
Poaceae indet.	8	47.1
Primulaceae	1	5.9
<i>Selaginella selaginoides</i>	1	5.9
<i>Silene acaulis</i>	1	5.9
<i>Taraxacum</i> cf. <i>alpinum</i>	1	5.9
cf. <i>Vaccinium uliginosum</i>	1	5.9
TOT	17	100.0

914
915
916

Table 1. Results of the plant macrofossil investigation: identified plant taxa within soil samples collected from the Umbric horizons in the soil profiles and from the soil-filled rock wedge.

917
918
919
920

Lab. Code	Sample ID	TOC (g/kg)*	Type	Radiocarbon Age (yr BP)	Cal. Radiocarbon Age (cal. yr BP) (2σ range)	Phase
LTL19173A	P1-1	19.0	Soil	7798 ± 75	8787-8434*	HCO
LTL19174A	P1-2	10.8	Soil	4918 ± 45	5744-5583	HCO
LTL19175A	P2-7	20.5	Soil	5639 ± 45	6500-6306*	HCO
LTL19172A	P2-8	11.0	Soil	7608 ± 75	8534-8302*	HCO
LTL19176A	P2-9	11.3	Soil	14203 ± 100	17536-17014*	ELID
LTL19542A	P2-9bis	12.5	Soil	14745 ± 70	18228-17870	ELID
LTL19169A	P3-2	8.7	Soil	15463 ± 100	18916-18611	ELID
LTL19543A	P3-3	10.6	Soil	17978 ± 120	22168-21431	LGM/ELID
LTL19170A	P3-5	11.8	Soil	11345 ± 65	13337-13110	BA
LTL19871A	P4	13.8	Soil	3820 ± 45	4405-4090	LH
LTL19865A	A	-	Plant	modern	After 1950 AD	M
LTL19866A	B	-	Plant	modern	After 1950 AD	M
LTL19867A	C	-	Plant	modern	After 1950 AD	M
LTL19868A	D	-	Plant	modern	After 1950 AD	M
LTL19869A	E	-	Plant	modern	After 1950 AD	M
LTL19870A	F	-	Plant	1789 ± 45	1796-1571*	RWP

921
922
923
924
925
926

Table 2. Radiocarbon ¹⁴C dating results of soil samples and plant fragments. HCO: Holocene Climatic Optimum; ELID: Early Lateglacial Ice Decay; BA: Bølling-Allerød; LH: Late Holocene; M: Modern; RWP: Roman Warm Period. *Total Organic Carbon (TOC) values derived from Pintaldi et al. (2021). *Weighted average age within the 95% confidence interval

Site	Elevation (m a.s.l.)	Cover type	$\delta^{13}\text{C}$ (‰)
S1	2840	Vegetation	-23.3
S2	2800	Vegetation	-25.1
S3	2770	Vegetation	-25.7
S6	2854	Vegetation	-23.4
S8	2749	Vegetation	-23.4
P4	3030	Vegetation	-22.7
P1-1	3030	Blockstream/Blockfield	-24.7
P1-2	3030	Blockstream/Blockfield	-23.9
P2-7	3030	Blockstream/Blockfield	-24.2
P2-8	3030	Blockstream/Blockfield	-23.9
P2-9	3030	Blockstream/Blockfield	-24.5
P2-9bis	3030	Blockstream/Blockfield	-24.5
P2-13	3030	Blockstream/Blockfield	-24.0
P2-15	3030	Blockstream/Blockfield	-24.3
P3-1	3030	Blockstream/Blockfield	-24.6
P3-2	3030	Blockstream/Blockfield	-23.8
P3-3	3030	Blockstream/Blockfield	-23.5
P3-4	3030	Blockstream/Blockfield	-24.0
P3-5	3030	Blockstream/Blockfield	-23.6

927
928

Table 3. IRMS $\delta^{13}\text{C}$ results of present-day vegetated soils in the study area and soils from the Plateau under blockstream/blockfield.